2022-02-03

Remote Sensing of Tundra Ecosystems using High Spectral Resolution Reflectance: Opportunities and Challenges

Nelson, PR

10.1029/2021jg006697
Journal of Geophysical Research: Biogeosciences
American Geophysical Union (AGU)

Remote Sensing of Tundra Ecosystems using High Spectral Resolution Reflectance: Opportunities and Challenges

Peter R. Nelson[1,*,‡], Andrew J. Maguire[2,*,‡], Zoe Pierrat[3], Erica L. Orcutt[4], Dedi Yang[5], Shawn Serbin[5], Gerald V. Frost[6], Matthew J. Macander[6], Troy S. Magney[4], David R. Thompson[2], Jonathan A. Wang[7], Steven F. Oberbauer[8], Sergio Vargas Zesati[9], Scott J. Davidson[10,11], Howard E. Epstein[12], Steven Unger[8], Petya K.E. Campbell[13], Nimrod Carmon[2], Miguel Velez-Reyes[9], K. Fred Huemmrich[13]

[1] Schoodic Institute at Acadia National Park, Winter Harbor, ME

[2] Jet Propulsion Laboratory, California Institute of Technology, Pasadena, CA

[3] University of California, Los Angeles

[4] University of California, Davis

[5] Brookhaven National Laboratory, Upton, NY

[6] Alaska Biological Research, Inc. Fairbanks, AK

[7] University of California, Irvine

[8] Florida International University, Miami, FL

[9] University of Texas at El Paso

[10] University of Plymouth, UK

[11] University of Waterloo, Canada

[12] University of Virginia, Charlottesville, VA

[13] University of Maryland Baltimore County, Baltimore, MD

‡ PRN and AJM made equal contributions

* Correspondence to:

Peter R. Nelson, pnelson@schoodicinstitute.org

Andrew J. Maguire, andrew.j.maguire@jpl.nasa.gov

Abstract

Observing the environment in the vast regions of Earth through remote sensing platforms provides the tools to measure ecological dynamics. The Arctic tundra biome, one of the largest inaccessible terrestrial biomes on Earth, requires remote sensing across multiple spatial and temporal scales, from towers to satellites, particularly those equipped for imaging spectroscopy (IS). We describe a rationale for using IS derived from advances in our understanding of Arctic tundra vegetation communities and their interaction with the environment. To best leverage ongoing and forthcoming IS resources, including NASA's Surface Biology and Geology mission, we identify a series of opportunities and challenges based on intrinsic spectral dimensionality analysis and a review of current data and literature that illustrates the unique attributes of the Arctic tundra biome. These opportunities and challenges include thematic vegetation mapping, complicated by low-stature plants and very fine-scale surface composition heterogeneity; development of scalable algorithms for retrieval of canopy and leaf traits; nuanced variation in vegetation growth and composition that complicates detection of long-term trends;

and rapid phenological changes across brief growing seasons that may go undetected due to low revisit frequency or be obscured by snow cover and clouds. We recommend improvements to future field campaigns and satellite missions, advocating for research that combines multi-scale spectroscopy, from lab studies to satellites that enable frequent and continuous long-term monitoring, to inform statistical and biophysical approaches to model vegetation dynamics.

Plain Language Summary

Remote sensing has a long history of characterizing the distribution and dynamics of vegetation in a wide variety of biomes, including the Arctic tundra which is experiencing warming more rapidly than the global average. Imaging spectroscopy (IS) - a rapidly advancing field of remote sensing that measures reflected light in narrow, contiguous “colors” from satellites, aircraft, or towers - has demonstrated great promise to “watch” how key land surface properties vary across space and over time. Because they are vast, remote, and have relatively little infrastructure, currently available IS data from the Arctic tundra are sporadic and intermittent. Hence, it has been challenging to study and characterize these ecosystems across broad spatial scales and through time. Furthermore, the climate and ecology of these ecosystems pose unique challenges for employing and interpreting IS data. Inspired by a forthcoming NASA satellite-based IS mission, we present an overview of the current opportunities and challenges for the use of spectroscopy to study Arctic tundra, informed by novel measurements across a range of spatial and temporal scales. We share recommendations for how researchers could leverage IS to resolve pressing ecological questions and advance the design and sampling scheme of future instruments and campaigns.

Key Points

- Imaging spectroscopy (IS) can help measure critical Arctic tundra properties, physiological function, and temporal dynamics
- Upcoming IS satellite missions including NASA's SBG will make imaging spectroscopy data widely available for Arctic tundra regions
- To properly interpret IS data users must consider spectral complexity of tundra driven by composition, sensitivity to climate, and phenology

1. Introduction

The Arctic tundra biome is of urgent and enduring scientific interest due to the rapid climatic and environmental changes occurring in this domain (IPCC, 2021) and the broad implications for ecosystems, Arctic people, and feedbacks to the global carbon cycle and climate system (Zhang et al., 2018). Because Arctic tundra ecosystems are vast, remote, and have relatively little infrastructure, it has been challenging to study and characterize them across large spatial scales (1 E4 km^2) and through time. Recent advances in imaging spectroscopy (IS)—remote acquisition of spatially co-registered images in narrow, spectrally contiguous bands (Schaepman et al., 2009)—have enabled unprecedented characterization of terrestrial vegetation across a range of biomes, and anticipated missions will soon enable regular and comprehensive spectral monitoring (Ustin & Middleton, 2021). The Arctic environment poses unique challenges and opportunities for the use of spectroscopy to help resolve uncertainties about the ecological sensitivity of the tundra biome and its response to a changing climate.

Recent years have seen the dramatic growth of spectral imaging studies in the Earth science and global ecology communities. The rapid technical progress of these methodologies has led to their designation as an integral part of the US National Aeronautics and Space Administration (NASA) new Earth System Observatory (ESO) set to launch in the 2027–28 timeframe. The Surface Biology and Geology (SBG) component of this observatory will include an imaging spectrometer in the solar-reflected range (400 - 2500 nm), with coverage at biweekly intervals and pixel size as fine as 30 m over the terrestrial and coastal aquatic areas of the globe. Combining these data with similar missions launching around the same timeframe, such as the European Space Agency (ESA) Copernicus Hyperspectral Imaging Mission for the Environment (CHIME) instrument (Nieke & Rast, 2018), will enable even denser spatial and temporal coverage. A key objective of the SBG mission is to use the solar-reflected spectrum to measure global ecosystem traits and diversity at high spatial resolution (Ustin & Middleton, 2021). Specific properties to be estimated from these data include plant traits, such as canopy nitrogen, leaf mass per area, liquid water content, and the fractional coverage of photosynthetically active (i.e., green) vegetation. By leveraging these data, specific plant functional types and canopy structures can be identified and mapped at the regional scale (European Space Agency 2021). With these new measurements, the forthcoming missions will provide the capacity to map ecosystem properties across the entire Arctic with unprecedented fidelity and temporal frequency - thereby serving as an important input to understanding Arctic ecosystem responses to a changing climate.

SBG measurements will complement a long history of prior airborne and *in situ* investigations of Arctic spectroscopy (e.g., Boreal Ecosystem-Atmosphere Study, BOREAS, and Arctic Boreal Vulnerability Experiment, ABoVE). These spectral measurements are often paired

with ground-based measurements of ecosystem characteristics, including flux towers with eddy covariance estimates of carbon dynamics. These local measurements and highly temporally resolved flux datasets are spatially sparse, which introduces uncertainties when upscaling to estimate Arctic productivity as a whole. Airborne observations, such as those from ABoVE, have mapped spectral surface reflectance over broad spatial extents, enabling trait maps for representative locales (Miller et al., 2019). These airborne data provide some capacity to fill the spatial gaps between study sites and flux towers but represent snapshots for a single point in time and therefore fall short of comprehensive temporal coverage (i.e., high frequency and long durations). Traditional multispectral broad-band satellite remote sensing (e.g., Landsat, MODIS) covers a broad spatial extent and multi-decadal period; however, these data cannot fully measure the broad suite of ecosystem parameters at the spectral resolution required for robust analyses of ecosystem structure, function, and responses (Beamish et al., 2020; Liu et al., 2017; Myers-Smith et al., 2020; Ustin & Middleton, 2021). SBG will rely on a long history of precursor investigations, but by combining imaging spectroscopy with spatiotemporal resolution akin to Landsat, the acquired data promise a unique and substantial advance in our capacity to understand Arctic ecosystems.

To realize this promise, SBG must overcome the challenges of spectroscopy in the Arctic environment, primary among them spatiotemporal scaling. Tundra ecosystems exhibit a high degree of sub-pixel heterogeneity in composition, structure, traits, and function that is consistent across high-altitude spectral imaging platforms with spatial resolutions typically > 5 m (Lantz et al., 2010; Niittynen et al., 2020). Underlying this heterogeneity is the small stature of most tundra vegetation, with individual plant canopies occupying centimeters to a few meters of space and characterized by compressed vertical structure (< 1 m). Vegetation cover in certain Arctic

regions is discontinuous with extensive exposed rock and soil. The widespread presence of permafrost and periglacial geomorphic features that produce fine-scale variation (< 0.1-10 m) in microtopography, soil moisture, and surface water exposure (e.g., ice-wedge polygons, frost circles, thermokarst features) contribute to this spatial heterogeneity of vegetation and terrain (Figure 1) (Li et al., 2021; Walker et al., 2003). Strong gradients in microclimate and topography yield a high degree of variance in physiological traits and function, even within individual species in close spatial proximity (Gamon et al., 2013; Kade et al., 2005). Thus, remote observations of tundra ecosystems usually integrate across a complex mixture of plant functional types, non-vegetated surfaces, and physiological traits.

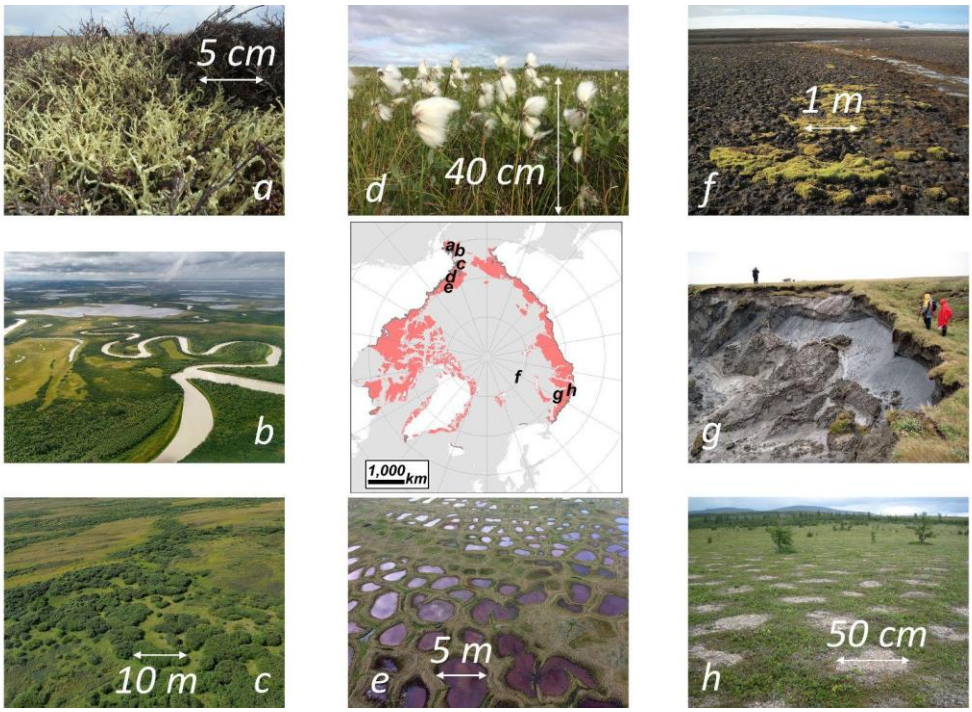

Figure 1. Examples of heterogeneous vegetation and landforms in tundra landscapes. (a) Close-up of ground lichens in upland tundra, Izaviknek Hills, Alaska; (b) mosaic of shrublands, wetlands, and waterbodies, Yukon Delta, Alaska; (c) mosaic of tall deciduous shrubs and open tundra, Seward Peninsula, Alaska; (d) intermixed sedges and low shrubs, Alaska North Slope; (e) polygonal ground, Alaska North Slope; (f) High Arctic tundra dominated by mosses and cryptogamic crust, Franz Josef Land, Russia; (g) thaw slump and exposed ground-ice, Yugorskiy Peninsula, Russia; (h) frost boils in forest-tundra ecotone, northwestern Siberia. The extent of the

Arctic tundra biome is shown in red in the central map based on the Circumpolar Arctic Vegetation Map (CAVM Team, 2003).

The composition of tundra includes significant coverage by both nonvascular and vascular vegetation. Nonvascular vegetation types pose unique challenges, in that they have different spectral signals than vascular plants (Hope & Stow, 1996; Stow et al., 1993) their spectra are highly influenced by their moisture content (Bubier et al., 1997; Harris et al., 2005; Vogelmann & Moss, 1993), and physiologically they behave differently than vascular plants (Green & Lange, 1995; Tenhunen et al., 1995). Relationships between remotely-sensed spectra and plant function have not yet been developed at spatial scales adequate to capture nonvascular plant physiological responses and the mixed composition of vascular and nonvascular plants within spectral footprints complicates interpretation of observations. Collectively, these issues suggest a need for multi-scale methodologies for assessing the composition of tundra systems. One approach is to collect collocated ground vegetation composition data and remotely sensed spectral observations at varying spatial scales, and utilize their relationships to enable subpixel vegetation cover retrieval (Thomson et al., 2021). Alternatively, spectral unmixing algorithms parameterized by observations at finer scales than the spatial resolution of imagery can be used to disentangle the sub-pixel contributions to a spatially integrated observation (Beamish et al., 2017; Bratsch et al., 2016; Huemmrich et al., 2013). Such work will be critical to interpret compositional effects on imaging spectroscopy observations from SBG - but present a major opportunity for future work.

Meteorological conditions inherent to Arctic regions, such as high frequency cloud occurrence, seasonal snow cover, and ephemeral surface water often preclude high quality spatially contiguous or temporally continuous observations (Walther et al., 2016, 2018). The

limited snow- and ice-free period (including episodic snowfall events in the middle of the growing season) constrains the number of clear observations of vegetation. Additionally, rapid transitions and highly variable shoulder season weather restrict the utility of even high frequency spaceborne observations to detect important phenological events (e.g., start-of-season and end-of-season) (Karlsen et al., 2021; Parazoo et al., 2018; Vickers et al., 2020). Smoke from frequent and extensive wildfires in the neighboring boreal forest biome can drift over the tundra biome for substantial periods during the growing season of a given year, making interannual comparisons challenging. Recent studies have successfully measured surface features under wildfire smoke with optical depths exceeding unity (Brodrick et al., 2021), but the suitability of these reflectances for vegetation analyses is unproven, and in practice even small amounts of smoke can distort trait or species retrievals.

Illumination geometry at high latitudes also complicates remote sensing of Arctic tundra (Buchhorn et al., 2016). High latitude regions experience extremes in daylength, from continuous daylight in midsummer to continuous darkness in midwinter, the latter of which limits the capacity for reflectance-based observations on the winter edge of shoulder seasons. The effects of the continuous daily photoperiod of midsummer challenge assumptions established in the temperate regions about the connections between spectral imaging observations and dynamic physiological processes (e.g., accumulated stress). Overall, surface radiation is lower due to high solar zenith angles and consequent scattering due to atmospheric path length, and photon scattering at such angles complicates radiative transfer.

Existing IS data over the Arctic is sporadic in space and time. For example, since 2017 ABoVE (Miller et al., 2019) has collected a large amount (> 1 E3 Tb) of airborne IS data over a broad Arctic region in North America using NASA's Next Generation Airborne Visible Infrared

198 Imaging Spectrometer (AVIRIS-NG). While these data are of high value for characterizing
199 vegetation function, stress, and mapping functional traits (Gamon et al., 2019), the discontinuous
200 coverage (non-overlapping flight lines collected over a larger region) and the volume of data
201 (several Gb in size for an individual flight line) mean that, at present, an individual researcher is
202 often required to identify and download a number of different scenes, and therefore a large data
203 volume (> 1 Tb), to carry out a study. Some of these challenges will be exacerbated with
204 upcoming satellite IS missions such as SBG (Cawse-Nicholson et al., 2021) which will provide
205 voluminous datasets. More efficient usage of IS datasets for Arctic research will require new
206 data hosting and access methods to find, extract, and apply IS data without large bandwidth or
207 local storage requirements.

208 Here, we present a technical perspective - informed by empirical observations of spectral
209 variability - of the numerous ecological, geographic, and technical challenges associated with
210 spectroscopic observation of Arctic tundra ecosystems. We discuss how we may leverage our
211 understanding of spectral dynamics and characteristics to understand tundra ecology. We delimit
212 our region of interest based on the Circumpolar Arctic Vegetation Map (CAVM Team, 2003)
213 (see Fig. 1). First, we provide context for the degree of spectral complexity of the tundra biome
214 using a relative qualitative metric of the intrinsic spectral dimensionality from a series of
215 observations from airborne IS (Section 2). Next, we describe how attributes of the land surface in
216 the tundra biome (e.g., plant functional type and vegetation-substrate composition) impose
217 challenges for interpreting spectroscopy (Section 3). We then elaborate on how IS enables an
218 opportunity to achieve several common goals for advancing our understanding of the Arctic
219 tundra biome: long-term change detection, land cover and vegetation classification, retrieval of
220 biophysical properties, and phenological and diurnal change (Section 4). We conclude by

providing recommendations for Arctic tundra spectroscopy research (Section 5) by addressing the following key questions:

1. How can we use spectral observations at a variety of spatiotemporal resolutions (e.g., from spaceborne, airborne, and surface-based instruments) to address inherent challenges associated with IS and better understand Arctic tundra ecosystems?
2. How can our understanding of Arctic tundra ecology advise further research and the development of new instruments and sampling designs?

2. Dimensionality Analysis

2.1. Intrinsic Dimensionality and Relevance to Arctic Optical Diversity and Ecosystems

Intrinsic dimensionality, the number of independent degrees of freedom in a dataset, has been used to measure the information content of spectral catalogues (Cawse-Nicholson et al., 2021; Thompson et al., 2017). The dimensionality indicates the diversity of different physical and chemical properties present on the land surface. Here, we characterize the differences in intrinsic dimensionality among different areas of the Arctic, as represented in the airborne ABoVE dataset acquired by AVIRIS-NG over Alaska and northwestern Canada. AVIRIS-NG is considered an imaging spectrometer, with 425 bands from 380 – 2510 nm sampled every 5 nm with spatial sampling ranging from 0.3 to 4.0 m. Our dimensionality analysis demonstrates that spectral diversity varies over short spatial scales (< 10 km) across the North American Arctic tundra highlighting the advantage of a large-scale experiment such as ABoVE and the increased information content provided by imaging spectrometers, as opposed to multispectral sensors.

2.2. Dimensionality Analysis Approach

We analyzed the AVIRIS-NG dataset acquired during the growing season (June – August) of 2017, consisting of over 200 different flightlines, segmented at ~3 km intervals (600 x 600 pixels at 5 m). The measured spectrum is calibrated to units of absolute radiance as in Chapman et al. (2019). We estimated surface reflectance spectra using the approach of Thompson et al. (2018). Finally, we calculated the intrinsic dimensionality of each segment independently using the strategy of Thompson et al. (2017). Within each segment, the intrinsic dimensionality was calculated from the image stack, cloud fraction and the mean and standard deviation of Normalized Difference of Vegetation Index (NDVI) were summarized from the imagery, and the central latitude and longitude were extracted. We plotted the frequency distribution of dimensionality for the cloud-free segments, summarized by latitude and NDVI, to examine trends and patterns in spectral dimensionality (Figure 2).

2.3. Dimensionality Analysis Results and Implications

Dimensionality was calculated for a total of 14,519 segments, of which 12,626 were cloud-free and used in subsequent analysis. Dimensionality values were positively skewed with a long tail of high values. Generally, a broad range of dimensionality was observed across the gradient of latitude and greenness. Above 62° N, segments with moderate NDVI values (0.25-0.75) consistently had higher dimensionality than those with either low (< 0.25) or high (> 0.75) NDVI. The lowest dimensionality values, < 20, were found mostly in the low NDVI category corresponding to non-vegetated terrain and open water. These systems were optically less diverse than the vegetated areas. Inconsistent observing conditions, such as solar angle and the amount of atmospheric haze, affect the sensor's ability to resolve the subtlest features and probably play some role in the broad spread of dimensionality values. Even excluding the largest

values, the modes of the distributions lie between 20 and 40. These numbers are broadly similar to previous studies of midlatitude grassland and needleleaf biomes (Thompson et al., 2017). However, a direct quantitative comparison with previous studies is inadvisable due to potential differences in sensors and acquisition conditions, as well as the spatial resolution of both the initial dataset and the analysis itself. Dimensionality analysis measures the information content measurable from a single sensor above its noise level; it is a qualitative metric which gives a sense of the spectral diversity within one particular study area. Because it depends on the instrument sensitivity, it is less useful for comparisons between studies. Regardless, this analysis indicates that different portions of the Arctic tundra exhibit spectral diversity that is considerably larger than that which could be measured using multiband sensors.

Unlocking the large amount of information available in these dimensions can provide new insights into tundra characteristics and function and will be the focus of future studies. Considering that this analysis was restricted to one segment size, it is quite likely that there is even more information embedded in these spectra. Dimensionality analyses like this conducted across a range of segment sizes and with coincident finer-grained data (< 5 m in this case) provide an important opportunity. Such analyses may be necessary to understand the properties of interest and heterogeneity across spatial scales within the mixture of non-vegetated and vegetated surfaces in the Arctic.

283

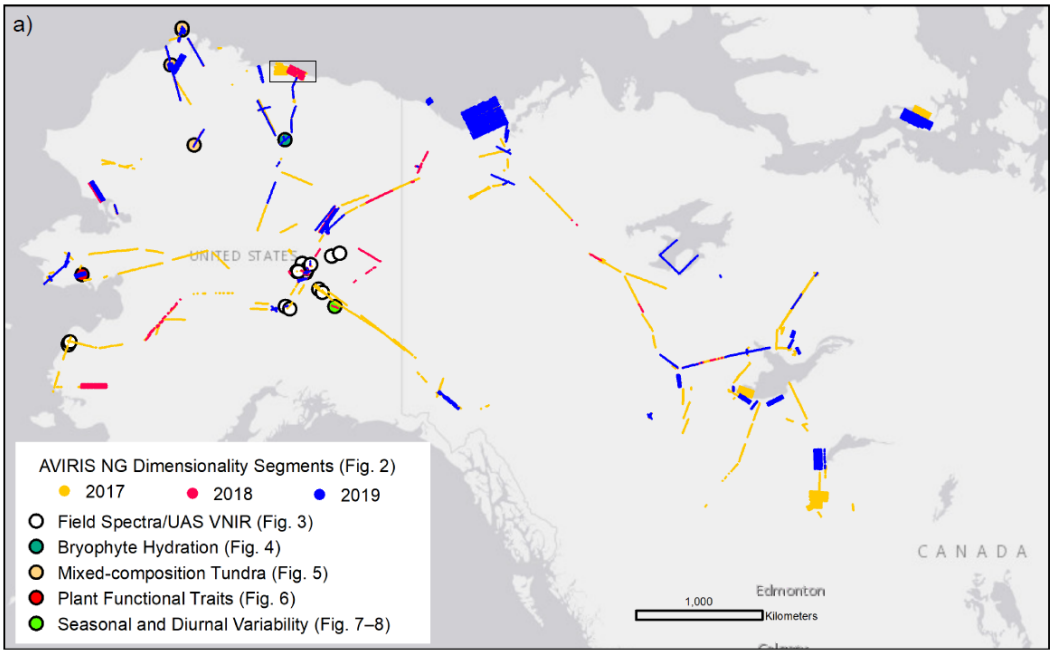
a)
UNITED STATES
CANADA
Edmonton
1,000
Kilometers
AVIRIS NG Dimensionality Segments (Fig. 2)
2017
2018
2019
Field Spectra/UAS VNIR (Fig. 3)
Bryophyte Hydration (Fig. 4)
Mixed-composition Tundra (Fig. 5)
Plant Functional Traits (Fig. 6)
Seasonal and Diurnal Variability (Fig. 7–8)

284

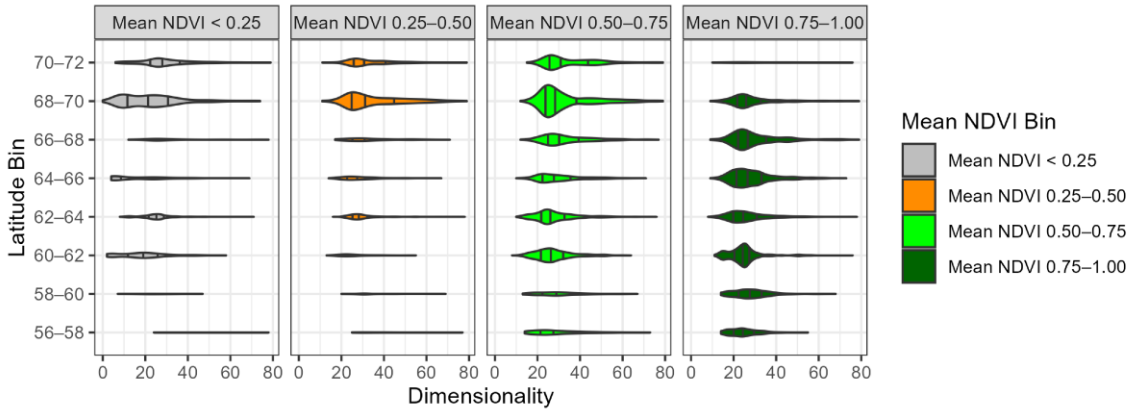
Mean NDVI < 0.25
Mean NDVI 0.25–0.50
Mean NDVI 0.50–0.75
Mean NDVI 0.75–1.00
Latitude Bin
70–72
68–70
66–68
64–66
62–64
60–62
58–60
56–58
0
20
40
60
80
Dimensionality
Mean NDVI Bin
Mean NDVI < 0.25
Mean NDVI 0.25–0.50
Mean NDVI 0.50–0.75
Mean NDVI 0.75–1.00

285

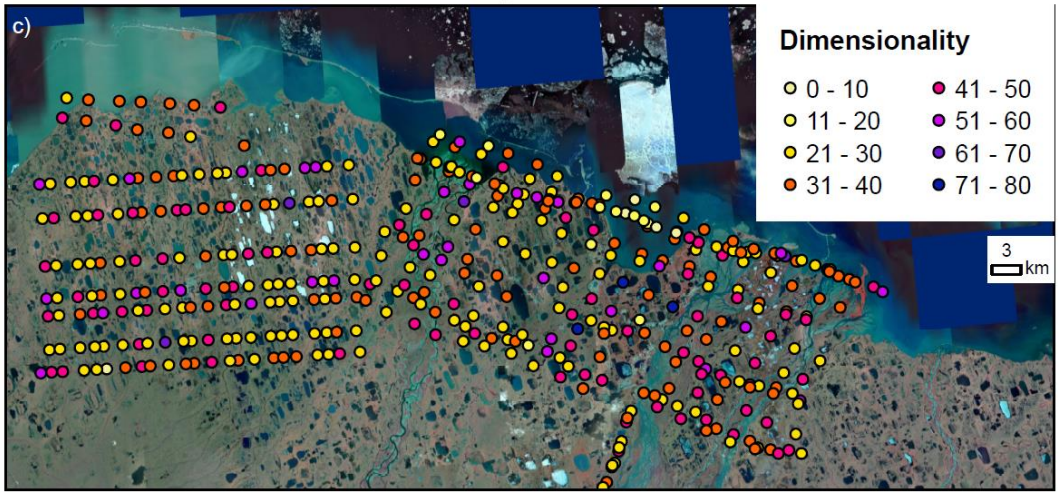
c)
Dimensionality
0 - 10
11 - 20
21 - 30
31 - 40
41 - 50
51 - 60
61 - 70
71 - 80
3
km

Figure 2. Locations of AVIRIS-NG flight line segments used in this analysis and ground-based measurements shown in Figures 3-8 are shown in the map (a). Frequency distribution from the dimensionality analysis, binned by latitude and mean NDVI (b). Vertical bars in the violin plots (b) indicate the inter-quartile range and median value. Map of AVIRIS-NG segments analyzed laid over satellite imagery in the Sagavanirktok River area of Alaska (area denoted by a black box in part (a)). Colors indicate the dimensionality ranges for the different segments.

3. Spectral Characteristics of Tundra

3.1. Characteristics of Tundra Surfaces

Lichens, bryophytes, and vascular plants occur in different proportions along gradients of climate, soil properties, and landscape history in the Arctic (CAVM Team, 2003; Epstein et al., 2008, 2020) and possess different physiologies and spectral reflectance patterns. This variability poses unique challenges for remote sensing of tundra vegetation properties, but an understanding of geographic patterns of vegetation structure and function can help interpret such measurements. Walker et al. (2005) provide a framework to characterize the central tendencies of Arctic tundra structure and composition by dividing the biome into five bioclimatic subzones (A–E) distributed along gradients of summer temperature. The subzones range from the coldest Subzone A, found in coastal areas of the High Arctic with persistent summer sea ice, to the warmest Subzone E, generally found in continental areas near the northern limit of tree establishment. Subzone A, occasionally termed “polar desert” (Matveyeva, 1998) is characterized by discontinuous vegetation cover that is typically dominated by nonvascular vegetation; shrubs and sedges are usually absent, vascular plant diversity is very low, and a large proportion of the ground surface is unvegetated. In Subzone B, lichens and bryophytes dominate the cover and shrubs are generally limited to only a few species (e.g., *Salix arctica, Dryas* spp.) with a prostrate growth form (< 5 cm height). From Subzone C southward, vascular plants -

311 particularly shrubs - occur at greater abundances and species richness, and of higher stature. In
312 Subzone E, vegetation is typically continuous and forms a multi-layered canopy, with shrubs
313 commonly reaching heights of > 80 cm. Near the southern boundary of Subzone E, broadleaf and
314 needleleaf trees are often present. The tundra-taiga ecotone (TTE) is typically a diffuse transition
315 zone where trees first occur as isolated patches within the tundra matrix and become more
316 abundant and spatially dense southward and at lower elevations. In North American and
317 European ecotones, tree cover is generally dominated by evergreen species (e.g., *Picea, Pinus*),
318 whereas deciduous needleleaf species (*Larix*) are dominant in Siberian TTE. Within each
319 bioclimatic subzone, there is a great deal of heterogeneity in the relative abundance of plant
320 functional types along landscape-scale gradients of moisture, topography, permafrost, and soil
321 properties. Thus, IS applications must consider the relative abundance of plant functional types
322 along both circumpolar-scale climate gradients and landscape-scale environmental gradients.

323 Furthermore, although plant functional types are expected to share suites of similar traits,
324 within plant functional types there can still be enormous variation among traits that are important
325 for ecosystem function (Table 1). This trait diversity corresponds to spectral variation within
326 individual plant functional types in (Figure 3).

327 **Table 1**. Summary of heights, patch sizes, dominant taxa, and distributional patterns of plant
328 functional types in Arctic tundra ecosystems and forest-tundra ecotones. For patch sizes,
329 minimum values refer to typical individual plants, and maximum values refer to contiguous areas
330 in which the functional type forms the top of the canopy.
331

Functional type	Height (cm)	Patch size (m^2)	Description & distributional patterns

Lichens	0–5	0.001–100	Diverse nonvascular plants consisting of fungal and algal symbionts, often distinguished by growth form (foliose, fruticose, crustose) or color group. Intermixed “reindeer lichens” (*Cladonia* spp.) and other fruticose taxa (e.g., *Flavocetraria, Alectoria,* and *Bryoria* spp.) can form extensive mats on undisturbed, well drained sites.
Bryophytes	0–5	0.001–100	Nonvascular plants including mosses and liverworts. Found throughout Arctic; common mesic taxa include branched “feathermosses” (e.g., *Hylocomnium splendens, Pleurozium schreberi*) and single-stemmed mosses (e.g., *Dicranum* and *Polytrichum* spp.). Peat mosses (*Sphagnum* spp.) can form continuous carpets in wet areas. Liverworts much less abundant, but form extensive cryptogamic crusts in High Arctic.
Graminoids	10–70	0.01–0.25	Sedges and grasses. Sedges common throughout tundra except in coldest parts of High Arctic. Tall cottongrass (*Eriophorum angustifolium*) and water sedge (*Carex aquatilis*) often dominate wet sites. Large areas of tussock tundra dominated by Arctic cottongrass (*Eriophorum vaginatum*) occur in Low Arctic on mesic soils. Grasses superficially resemble sedges and occur throughout Arctic, but cover is usually low; most common on floodplains and disturbed sites. Pendantgrass (*Arctophila fulva*) is a common marsh species.
Forbs	0–50	0.01–0.05	Diverse group of non-graminoid herbaceous flowering plants found throughout the Arctic, but cover is typically low. Common forbs include Arctic lupine (*Lupinus arcticus*), Arctic sweet coltsfoot (*Petasites frigidus*), and “cushion” plants such as purple mountain saxifrage (*Saxifraga oppositifolia*).

Deciduous shrubs	0–500	0.01–100	Multi-stemmed, broadleaf woody plants; common erect species include dwarf birch (*Betula nana*), diamondleaf willow (*Salix pulchra*), and bog blueberry (*Vaccinium uligonosum*). Dwarf shrubs such as Arctic willow (*Salix arctica*) occur throughout tundra biome except in coldest parts of High Arctic. Tall stands are restricted to warmer parts of Low Arctic, where typically found on floodplains (e.g., feltleaf willow *Salix alaxensis*) and mesic slopes (e.g., Siberian alder *Alnus viridis* ssp. *fruticosa*).
Evergreen shrubs	0–20	0.01–10	Widespread dwarf shrubs, except in High Arctic. Common species include entireleaf mountain-avens (*Dryas integrifolia*), mountain heather (*Cassiope tetragona*), lingonberry (*Vaccinium vitis-idaea*), and Labrador tea (*Ledum decumbens*).
Deciduous trees	150–1,000	1–25	The deciduous conifer, larch (*Larix* spp.), is the dominant tree in Siberian taiga-tundra ecotones. Poplar (*Populus balsamifera*) can occur on Low Arctic floodplains and south-facing slopes. Trees are typically widely spaced. Conifers typically have columnar growth form with small canopies; broadleaf trees often have larger canopies.
Evergreen trees	150–1,000	1–10	Evergreen conifers such as spruce (*Picea* spp.) are dominant in North American and European taiga-tundra ecotones.

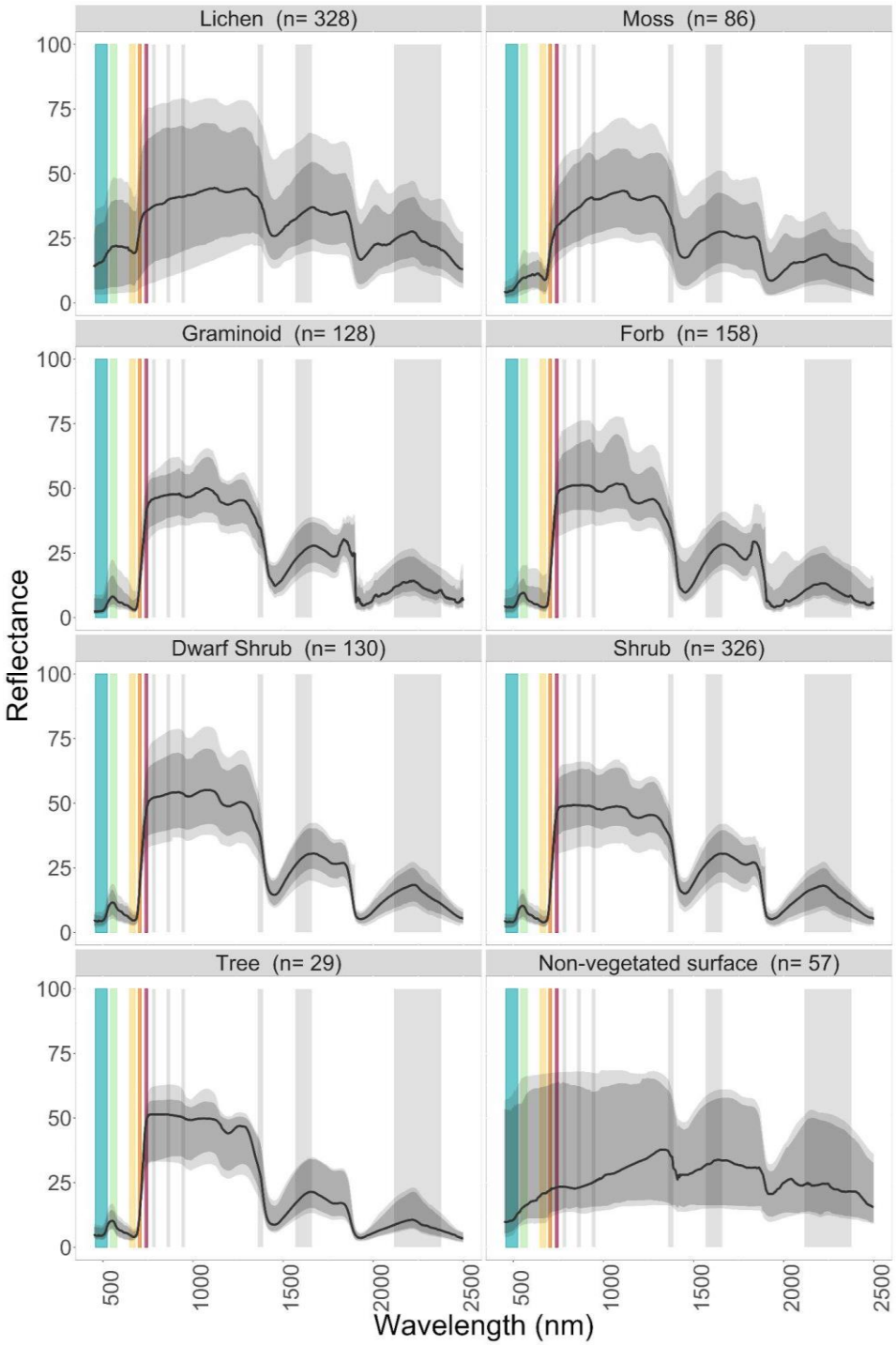

Figure 3. Median (black), 75% (dark ribbon), and 90% (grey ribbon) quartiles of spectral reflectance for eight plant functional types from the Arctic tundra biome. Sample size (*n*) is shown parenthetically. Sentinel-2 bandpasses are indicated with colored vertical bars to illustrate the advantage of imaging spectrometers with contiguous bands over multispectral instruments. Spectra were collected in the field with leaf clip or contact probe and illumination source across Alaska between 2010-2019, primarily 2017-2019. Most of the data were collected with a Spectral Evolution PSR+3500 under AVIRIS-NG flight lines +/- 14 days of flight in most cases.

Spectra were collected at 1 nm resolution and trimmed to 450-2400 nm to remove sensor artifacts.

3.2. Lichens

Lichens reach high diversity, cover, and biomass in certain tundra ecosystems and play a significant role in biogeochemical and physical processes, such as land-atmosphere radiative exchange, hydrological buffering, and nitrogen (N) cycling (Cornelissen et al., 2007). The genus *Cladonia* (reindeer lichens) create dominant carpets across the Arctic that likely represent the majority of lichen cover and biomass. Other genera do contribute significant biomass and cover, such as *Cetraria*, *Flavocetraria* and *Stereocaulon* all which grow mostly upright and intermixed with bryophytes, lichens and other plants. However, talus slopes and other rock surfaces are often covered with very different genera (eg. *Rhizocarpon* and *Aspcilia*, both crustose or stain-like growth forms that can cover boulders and talus fields), which creates complexity in estimating the total cover of lichens. Lichens contribute substantial ground cover in periglacial environments, stabilizing soils (Makoto & Klaminder, 2012). Albedo varies widely among lichen groups, with implications for heat exchange with fractional cover variability (Aartsma et al., 2021). A large fraction of biodiversity of terrestrial vegetation in the tundra is composed of lichen species. Most caribou and reindeer survive in northern climates, in part, by eating mostly lichens throughout winter months (Heggberget et al., 2002; Joly et al., 2007). A major opportunity for SBG to enhance wildlife habitat mapping will be to use the unique spectral signatures to separate lichen groups (Macander et al., 2020; Nelson et al., 2013; Petzold & Goward, 1988; Rees et al., 2004).

Physiological differences between lichens and vascular plants affect their spectral reflectances. Lichens have more broadly different cellular structure than vascular plants. The upper surfaces of most lichens, composed of fungal cells of one or sometimes two fungi (Spribille

et al., 2016), often with pigments, protect the next inner layer of cells, usually composed of the photobiont (algae, cyanobacteria, or both). The upper cortical cells of lichens are usually dense and have high concentrations of pigments produced by one or both fungi that are attributed to photoprotection. These fungal pigments protect the algal photosynthesis machinery by dealing with reactive oxygen species produced by high irradiance by dissipating excess energy as thermal wavelengths (Beckett et al., 2021). Under the cortex, a thin layer of photobiont (algae, cyanobacteria, or both) receives sufficient light for photosynthesis. The parts of the spectral signature of lichens similar to vascular plants belies the presence of the photobiont(s). After the photobiont, little if any light likely penetrates in the fungal structural backbone of a lichen body, the medulla, which is often thick, white or pale. Amongst the > 12,000 species of lichens, there is a diversity of mixtures of cortical cell structure, chemistry and photobiont that contribute to the spectral signatures of lichens.

Lichens are spectrally variable both within and among species, but compared with vascular plants, tend to have higher reflectance in the visible range and lower reflectance in the NIR (Figure 3). Hundreds of compounds, many with pigments detectable in the visible range, can be found across the diversity of tundra lichens. These complex molecules aid in differentiating lichens from vascular plants but also make modeling lichens as a group difficult. However, most mapping efforts have treated lichens as a monolithic group, focused on one relatively homogenous color group (e.g., light) (Macander et al., 2020) or at most treated lichens in a few color groups (Nelson et al., 2013). Lichen spectral signatures indicate high degrees of variability within and among species (Kuusinen et al., 2020; Petzold & Goward, 1988; Rees et al., 2004). Lichens have no true vascular tissue therefore hydration is based on short term meteorological conditions (hourly) which in turn drives short term metabolic activity of lichens (Lange et al.,

1996). Nonvascular plants, including lichens and bryophytes (i.e., mosses, hornworts, and liverworts), lack true vascular tissue (parenchyma) and therefore passively desiccate and rehydrate (poikilohydry) (Walter, 1931). The hydration status of lichens greatly influences the overall magnitude of reflectance as well as spectrum shape (Kuusinen et al., 2020; Rees et al., 2004) but the difference between dry and wet lichen spectra varies both across wavelengths and species. Water content can be estimated for lichens (Granlund et al., 2018) but uses wavelengths beyond those proposed for SBG (i.e., > 5000 nm). A key challenge for SBG in the Arctic will be accounting for water content in spectral profiles of the lichen (and bryophyte) mat since photosynthesis and respiration are both tied to hydration. Rapid changes in hydration make observations of productivity fleeting and unstable in non-vascular plants. To address the impact of hydration state on the reflectance profiles of non-vascular plant communities, diurnal and seasonal spectral measurements with high temporal density collocated with in situ moisture probes are needed.

Lichens tend to be very small organisms but, in the tundra, can form confluent patches of varying sizes (~100 m^2) and mixtures of patches with different species and other organisms. Studies of tundra with coincident imagery of different spatial resolutions suggest pixels smaller than 3 m are needed to accurately classify patches (Räsänen & Virtanen, 2019) with a loss of 30% absolute accuracy associated with declining resolution (2-20 m) (Virtanen & Ek, 2014). Another key challenge for leveraging observations from SBG will be the fact that the composition of surfaces in 30 m pixels will have a wide range of pure patch sizes, from centimeters to meters.

There are few measurements on the phenology of pure lichen patches. Measurements of tundra mixtures with abundant lichens display limited seasonal variability (Gamon et al., 2013) with spectral changes mostly associated with moisture status. This may be one of the few positive

features of lichens for remote sensing and SBG. To take advantage of this, SBG could use observations after snow melt but before green up and then after leaf-off but before first snow to observe lichen (and bryophyte) dynamics in more detail. At those times, non-vascular vegetation would have less over-topping vegetation, reducing occlusion from nadir-viewing sensors.

3.3. Bryophytes

One of the main features of the tundra are the bryophytes, which can be found growing on most surfaces and conditions, from fully immersed in water to exposed rock or bare soil. Bryophytes (i.e., mosses, hornworts, and liverworts) usually appear as mats or patches of miniature plants formed by multiple individuals. Bryophytes can form the primary understory vegetation in many tundra plant communities, from wet, acidic bogs where *Sphagnum* spp. Dominate to the fine matrix of moist tundra where numerous species of bryophyte form dense mats interspersed with lichens and vascular plants. In wet environments, *Sphagnum* spp. Can create large colonies (100 m^2) with deep accumulation of senescent material storing carbon as peat. In less hydric sites, *Hylocomium splendens* (stair step moss) and *Pleurozium schreberi* (big red stem) are dominant. They have exceptional hydrologic and thermal buffering qualities and are tied to the formation and stability of permafrost (Blok et al., 2011; Shur & Jorgenson, 2007). Bryophytes such as *Polytrichum* spp. And *Ceratadon purpureus* can also form short-lived (annual) but extensive colonies post-fire which aid in stabilizing carbon recovery. They are crucial to carbon sequestration and storage, protecting the permafrost layer while also forming a living layer beneath a sparse vascular plant canopy. Despite their obvious importance to Arctic ecosystems, bryophytes have been largely neglected in remote sensing except for narrow cases like *Sphagnum* spp. (Angela Harris & Bryant, 2009; Huemmrich et al., 2013).

Bryophyte physiology differs vastly from vascular plants, primarily due to reduced-to-absent vascular tissue. By virtue of this, bryophytes can absorb large amounts of water (> 100% of dry mass), but are not able to actively regulate moisture content via a root system like vascular plants. Instead, bryophytes form colonies, sometimes only with one species but often with many species, which together determine hydration through water holding capacity of the living layer. As a result, bryophytes may hydrate or desiccate quickly. Similar to lichens, bryophyte hydration status is known to significantly influence spectral reflectance, with many changes observable in the visible to short-wave infrared spectra (Van Gaalen et al., 2007; Vogelmann & Moss, 1993) (Figure 4).

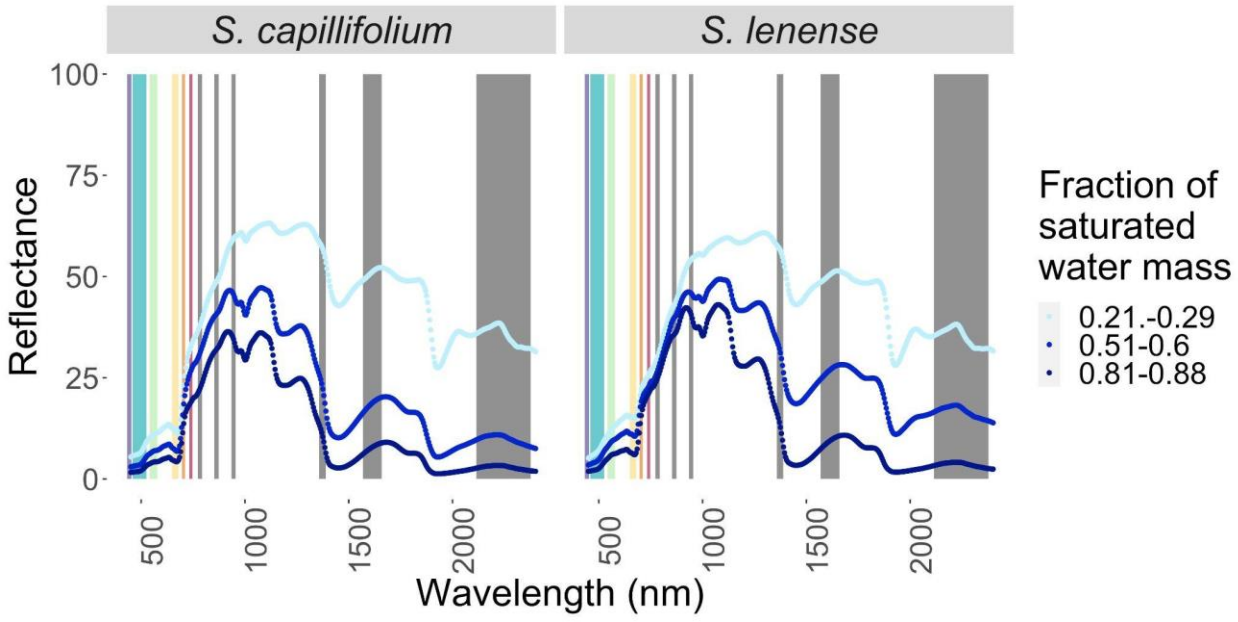

Figure 4. Spectral signature at varying moisture saturation levels measured as a fraction of the saturated water mass of *S. capillifolium* (left) and *S. lenense* (right). Spectra for both species were collected at regular intervals using a SVC – HR-1024i with light source at 100% under a progressive drying experiment. Fraction calculated as mass of water in samples divided by total water mass (g H_2O at interval * g total H_2O^{-1}). Sentinel-2 bandpasses are indicated with colored vertical bars to illustrate the advantage of imaging spectrometers with contiguous bands over multispectral instruments.

In addition to spectral changes, metabolic activity of bryophytes is also significantly influenced by moisture content with primary production decreasing as moisture decreases (Green & Lange, 1995); however, decoupling of reflectance and productivity has been noted in *Sphagnum* spp. And Pleurocarpous mosses, such as *Hylocomium splendens* and *Pleurozium schreberi* with spectral indices such as NDVI returning to near-initial values within minutes after rehydration, but primary production response lagging for more than 24 hours (May et al., 2018).

Given the generally low canopy cover across the arctic, bryophytes are likely driving spectral reflectance of mixed pixels, making timing of data collection and awareness of moisture content crucial for interpreting IS observations. For this reason, early and late summer provide opportunities for IS of bryophytes. Though there are many lab studies of bryophyte physiology (Green & Lange, 1995), the few studies scaling bryophyte spectral signatures for classification and chemical analysis show promise for estimating water, N, C, and P (Thomson et al., 2021). Translating bryophyte spectra to trait maps using remote sensing is an important opportunity to better constrain ecosystem models (Wullschleger et al., 2014).

Bryophyte reflectance spectra differ from vascular vegetation by exhibiting a wider and taller peak in the green to yellow, a gentler red edge, and a greater variability in the NIR (Figure 3). Additionally, the SWIR region is very responsive to moisture content with large increases (> 2x) in reflectance under drier conditions. Bryophytes also produce photoprotective compounds that influence the spectral profiles. For example, many *Sphagnum* species under high light conditions may develop photoprotective pigments that will affect their reflectance. Studies of open-growing *Sphagnum* have shown that they are photo-inhibited in full sun and exhibit faster vertical growth under lower (e.g., shaded) illumination (Harley et al., 1989; Murray et al., 1993). Little is known about the variability of pigments among bryophytes species across the extent of the Arctic.

Reflectance measurements *in situ* indicate broad diversity both within and among bryophyte species that will be further complicated by the impact of variable hydration status.

Though short in stature, bryophytes can form small but highly visible homogeneous patches (~100 m^2), carpets and hummocks. Bryophyte mixtures are very commonly intermixed with vascular plants (dwarf shrubs and grass-like plants) and lichens, in the understory living-mat matrix. The mixtures of patch sizes of each species and degree of heterogeneity combined with vascular plant canopy cover make it challenging to separate them spectrally. Similar to lichens, classification accuracy of bryophytes can be high if pixels are small (< 1 m) and there are sufficient and appropriate bandpasses (Räsänen & Virtanen, 2019). For context, researchers found that increasing to 20 m pixels reduced the absolute accuracy of their plant classification of remotely sensed spectra by 50% compared to 2 m pixels (Thomson et al., 2021). Like lichens, small patch sizes of bryophytes present a challenge for SBG that will need to be met with scaling studies to understand within-pixel variation.

Bryophytes generally do not display strong seasonal patterns in their reflectance, although there are few studies of pure bryophyte patch phenology. Vegetation classes with high fractional cover by bryophytes do show some phenological variability but this is likely primarily due to the non-bryophyte fraction in the vegetation class (Rautiainen et al., 2011). In the spring, following snowmelt, bryophytes are green and photosynthetically active well before the deciduous vascular plants begin greening up (Huemmrich et al., 2010). New annual growth of many bryophyte species appears much lighter green than older growth. Bryophytes in shaded vs open areas also show different chlorophyll and other pigment concentrations (Niinemets & Tobias, 2014). Bryophyte reproductive structures develop annually in many species and these tissues display apparent coloration distinct from the vegetative tissue. Bryophyte phenological variation may

occur at scales at which IS could be useful in detecting physiological changes relevant to ecosystem processes.

3.4. Vascular plants

Living vascular plant tissue shows remarkable similarities as a group in the general shape of spectral response, specifically characterized by a modest increase in reflectance in the green (relative to blue and red) and a steep "red edge," followed by a plateau across the NIR (Figure 3). Variation in spectral profiles among vascular plants is often most notable in the inflection point of the NIR and features of the SWIR, which in turn inform the derivation of many important functional attributes (e.g., phenology, photoprotective pigmentation, water content, disease). Spectral profiles are evolutionarily conserved (Meireles et al., 2020), which provides a basis for assuming the ability to separate species using spectra. Reflectance profiles have recently been used to separate species and even genotypes among co-occurring plants (e.g., *Dryas* sp., one of the most common vascular plant genera in the Arctic) (Stasinski et al., 2021). This level of distinction is likely beyond the capacity of SBG but points to the profoundly strong linkage between vascular plants and their reflectance profiles.

Vegetation in the Arctic occurs largely in confluent mixtures, where the boundary between an individual and group blurs. Viewing this problem in terms of pure patches of a single species helps describe the challenge for remote sensing. Patch size varies by species across several orders of magnitude, from individual plants (cm scale) to confluent forest or shrub canopies (10 m scale) or continuous patches of a single type (km scale) such as tussock tundra dominated by *Eriophorum vaginatum*. Snow, wind and ice scour the landscape and force shrubs to form thickets that can cover thousands of m^2 but change in size and shape across species of dominant

shrubs, like *Salix* spp. (willows) or *Alnus* spp. (Alder). The sparse distribution of trees presents unique challenges to spectral remote sensing, particularly for coarse spatial resolution imagery where tree crowns may be widely spaced and collectively constitute on average 30% of a 30 m pixel (Montesano et al., 2016). In contrast, some regions of the TTE are characterized by clumps of dense tree cover with minimal spacing between crowns across otherwise open tundra vegetation. As with non-vascular plants, many vascular plant patches are smaller than the likely pixel size of SBG (30 m). This underscores the need to measure features at high spatial and spectral resolution with coordinated field campaigns to validate SBG pixels and fully utilize the spectral resolution of SBG to estimate vegetation composition and function.

Vascular plants exhibit strong variation in phenology across groups, from fully dormant species such as forbs that are absent aboveground or buried under snow in the winter to persistent year-round tissues of evergreen trees and shrubs. The brief growing season results in very rapid progression of plant phenological stages, which elicits the common perception by observers that changes in reflectance are visually apparent at a daily time scale. Most studies have focused on summer reflectance for peak photosynthetic activity, but imaging at other times of year provides opportunities to characterize the important features of green up and senescence. For most plants snowmelt defines the onset of annual growth and initiation of myriad phenological processes including flowering and leaf-out. Characterizing differences in phenology among plant functional types may help separate co-occurring plant groups with similar reflectance profiles during peak summer (Beamish et al., 2017). Spatial variation in onset of green up (earlier at lower latitudes, south facing aspects, and lower elevations) and senescence (earlier at higher latitudes, north-facing aspects, and higher elevations) provides both a challenge and an opportunity for SBG to capture the important spectral information about the biophysical

changes in tundra vegetation. In shoulder seasons when understory vegetation is buried under snow but tree crowns protrude above the snowpack, lower albedo distinguishes these patches from surrounding snow-covered tundra. However, to detect phenological events in sparsely treed regions, indices that can account for background effects – namely the coincidence of snow with vegetation phenology – are critical (see Section 4.4).

Vascular plants generally become increasingly important, more diverse, and larger with decreasing latitude and altitude in the Arctic. By subzone C and south vascular plants become more prevalent than nonvascular plants, with increasing diversity of growth forms/functional types, graminoids, forbs, cushion plants, and deciduous and evergreen shrubs and trees that represent general life history strategies characterized by specific traits (with many exceptions) that influence ecosystem and spectral properties. For example, evergreen shrubs and trees are characterized by long-lived leaves (years), low photosynthetic rates, low leaf nitrogen but high leaf mass per unit leaf area (LMA), and tolerance to water stress. Forbs and deciduous shrubs tend to have short-lived leaves (annual), high photosynthetic rates and leaf nitrogen contents, and low LMA. Graminoids may span the entire spectrum.

Graminoids (mainly sedges) form a large component of boreal and tundra herbaceous vegetation, ranging from dry ridges to wet areas and standing water. Reflectance profiles of graminoids are broadly similar to other vascular plants with some distinctive features in the SWIR and overall lower green values. However, fine-scale spatial mixtures (0.1-1 m) of living and dead tissue in graminoid end members present a different spectral challenge for remote sensing. Collecting clean graminoid spectral signatures in the field under controlled light conditions is difficult due to the shape and size of the leaves. For this reason, most measurements

563 of graminoids in the field are taken with a larger FOV under ambient and therefore often have
564 dead leaves and stems that remain mixed in with living graminoid tissue thereby creating the
565 mixture of living and dead tissue in the spectral profiles for this group.

566 The tussock-forming sedge *Eriophorum vaginatum* (cottongrass) is a dominant species over
567 very large areas throughout the Arctic (0.9×10^6 km^2; Oechel et al., 1993). Its unique tussock
568 growth form provides an unusual surface topography that introduces shadows and at low
569 observation angles may obscure vegetation on the opposite side. Cottongrass and many other
570 graminoid species also have predominantly vertically-oriented leaves that present a challenge for
571 top-down, nadir remote sensing because most of the leaf area is not apparent to the sensor;
572 further. Again, a key challenge for remote sensing of graminoids will be accounting the amount
573 of dead material in spectral profiles of these plants.

574 Forbs are the dominant vascular plants in snow banks and snow beds, where the annual
575 growing season is brief but water and nutrient supplies are high and present in dry to semi-
576 aquatic habitats throughout the Arctic. They are non-woody non-graminoids that typically
577 present only leaves and flowering stalks above the soil surface during the growing season. Forbs
578 show broad similarity to shrubs in their spectral profiles, but with more variability in the visible
579 range and more symmetrical variation about the median in the SWIR (Figure 3). Separating forbs
580 from other vascular vegetation may be a challenge for SBG but one opportunity may be during
581 the autumn, when the spectacular variation in pigments of Arctic tundra forbs and dwarf shrubs
582 becomes strikingly apparent.

583 The expansion of deciduous shrubs is one of the most apparent responses of tundra
584 ecosystems to climate warming. Deciduous shrub species have high environmental plasticity and
585 are unique among tundra plant functional types in the Low Arctic, because they can achieve

586 canopy heights of 2 m or more and greatly overtop other vascular plants. Therefore, the
587 development of upright, woody canopies in tundra landscapes strongly influences biophysical
588 processes throughout the year. Shrubs promote a strong positive winter feedback by trapping
589 drifting snow in the winter that insulates the soil; subsequently warmer soils allow faster
590 decomposition; decomposition releases nutrients that promote further shrub growth (Sturm et al.,
591 2005). In warmer parts of the Low Arctic, the large size attained by individual deciduous shrubs,
592 and their tendency to develop dense canopy patches in favorable landscape positions provides
593 opportunities for IS to sample a relatively pure spectral signal, which is otherwise not possible in
594 most tundra landscapes dominated by small, intermixed, low-statured plants (< 1 m). Deciduous
595 shrubs exhibit limited variation in the visible range and a notable plateau in the NIR (Figure 3).

596 Evergreen shrubs present a different set of challenges and opportunities for IS. In moist
597 acidic and dry tundra, dwarf evergreen shrubs are a major component of the vegetation, often as
598 an understory layer above bryophyte species (e.g., *Vaccinium vitis-idaea* L.). The evergreen
599 growth form is associated with low nutrient habitats where conservative use of nutrients is
600 favored. Evergreen shrubs retain leaves for 1-5 or more years (Shaver, 1981) and thus have the
601 potential to photosynthesize whenever conditions are able to sustain it, even under snow (Starr &
602 Oberbauer, 2003), especially during the shoulder seasons. Most evergreens produce
603 photoprotective pigments that protect the leaves during the cold season and strongly affect
604 spectral reflectance of these plants (explored further in section 4.2).

605 Even in otherwise tundra-dominated landscapes, trees can persist in sparse numbers across
606 the tundra domain. The primary example of this is along the tundra-taiga ecotone (TTE), which
607 is an often diffuse (rather than abrupt) transition between denser boreal forest tree cover to
608 tundra-dominated plant cover. Common tree genera of the TTE include a mix of evergreen

609 needleleaf (e.g., *Picea* and *Pinus*), deciduous needleleaf (e.g., *Larix*), and deciduous broadleaf
610 (e.g., *Betula and Populus*). Having more structural complexity than forbs, bryophytes, or lichens,
611 trees exhibit different effects on radiative transfer within canopies, particularly affecting multiple
612 scattering in the NIR and SWIR regions. For example, conifer needles have similar reflectance to
613 deciduous in the VNIR, but their IR reflectances are lower than deciduous due to morphological
614 characteristics of needles (Hovi et al., 2017). Observed and simulated radiative transfer of
615 conifer needles infer that part of the spectral differences between deciduous leaves may be due to
616 variation in leaf angle with both convex and flat leaf sides to their needles (J. Wang et al., 2020).
617 Conifer arrangement in shoots, and the presence of woody material in twigs and boles that alter
618 multiple scattering likely also differs between deciduous trees. Evergreen needleleaf trees in the
619 TTE tend to have exceptionally narrow crowns (maximum 1-2 m in diameter), and black spruce
620 (*Picea mariana*) can often have sparse foliage clustered at the top of the crown, especially in
621 regions where fire had caused non-lethal disturbance. Due to their upright structure and tendency
622 to be widely spaced in much of the TTE, the interaction of high solar zenith angles with tree
623 stems and canopies cast extended shadows on surrounding tundra vegetation. The vertical
624 distribution of foliage along narrow crowns causes problems for nadir viewing of trees in the
625 TTE to characterize gradients in foliar properties (Moorthy et al., 2008). In addition to the
626 structural complexity of trees, deciduous vs. evergreen species experience strong phenological
627 differences which may complicate interpretation of spectral information in mixed-forest stands
628 (Pierrat et al., 2021) (Section 4.4). As with shrub-dominated landscapes, understory tundra
629 vegetation may be obscured from measurement by nadir-viewing sensors in regions with denser
630 tree cover. Similar to the case of shrubs, encroachment of trees into tundra landscapes influences
631 biophysical processes such as snow distribution, wind patterns, and soil active layer depth (F. K.

632 Holtmeier & Broll, 2007). Characterization of geographic position, composition, and condition
633 of the TTE is important for detecting expansion or retreat of tree species across the tundra
634 domain (Holtmeier & Broll, 2019; Montesano et al., 2020; Stumberg et al., 2014).

635 Though lidar is often the primary tool for delineating the TTE and characterizing the
636 structure of trees in this zone, spectroscopy can provide valuable information on phenology,
637 physiological state, and heterogeneity among trees (Montesano et al., 2016a; Montesano et al.,
638 2016b). Spectroscopy is particularly useful for characterizing photosynthetic dynamics of trees in
639 the tundra domain since these individuals tend to be especially slow growing at the northern
640 range limit for their species distribution (hence limited structural change detectable by repeated
641 lidar campaigns) but contribute a substantial amount to landscape-scale carbon flux.

642 **3.5. Non-vegetated Surfaces**

643 The Arctic tundra is characterized by low leaf area and sparse vegetation cover, resulting in
644 other materials, such as snow, water, bare ground, and dead or burned material comprising
645 significant portions of the landscape. Each of these materials have unique spectral characteristics
646 which can confound retrievals of vegetation. Remote sensing instruments with fine to moderately
647 sized pixels (e.g., AVIRIS-NG ~ 5 m^2) can capture multiple landscape components within a
648 single pixel, producing a mixed spectral signal that can be difficult to interpret. Our ability to
649 tease apart vegetation signals from these non-vegetated tundra landscape components is
650 important not only for understanding vegetation, but also for understanding the condition of the
651 landscape itself and its feedbacks on vegetation dynamics. An additional complication is that
652 many surfaces are non-vegetated for only part of the year due to snow pack, snow melt, or
653 flooding; at other seasons understory vegetation in the form of lichens, bryophytes, or biocrusts

becomes visible from above making the timing of signal retrievals an important component of Arctic vegetation dynamics.

Remote sensing of the cryosphere has been a key focus of Arctic remote sensing. Snow, ice, and permafrost are important drivers of tundra ecosystem structure and function, impacting components such as the depth of the soil active layer, freshwater availability, and the formation of important landscape features such as thermokarst lakes. Fresh snow has very high reflectivity in the visible and near-infrared (> 80% between 400 – 900 nm, with values > 50% between 900 – 1200 nm), while clean ice, as from a glacier, has relatively high reflectivity (> 60% between 400 – 600nm, steadily decreasing to < 10% for 1000 – 1200 nm) (Tedesco, 2015). The reflectivity of ice and snow is reduced over time as dirt accumulates and darkens the surface. Snow can interfere significantly with vegetation spectral retrieval as snow can both accumulate over vegetation canopies (i.e., obscuring direct visibility) and snow reflectance can saturate any vegetative signal. The timing of snowmelt, a key driver of tundra phenology, can vary drastically throughout the tundra (Kelsey et al., 2021), making snow dynamics both an important process to study but also a confounding factor in vegetation remote sensing (further explored in Section 4.4).

Permafrost thaw in the Arctic tundra is one of the most concerning results of climate change due to the biogeochemical feedbacks which drive increased greenhouse gas emissions. The spatial dynamics of permafrost thaw are complex, involving interactions between multiple processes including biogeochemical cycles, hydrology, and climate (Grosse et al., 2013). Vegetation cover can provide insulation from summer warming, with different types of cover providing varying levels of protection against thaw, which makes vegetation change detection an important component of understanding permafrost thaw changes (Anderson et al., 2019).

Vegetation feedbacks between the permafrost and vegetation provide a key geophysical connection for SBG in studying the Arctic because the high spectral resolution will allow separation of more kinds of tundra attributes. However, permafrost features have highly patterned features, often considerably finer scale than the 30 m resolution of SBG, requiring field campaigns to describe patterns in the permafrost at higher spatial resolution. Permafrost thaw can also impact vegetation cover through landscape transformation.

One of the most rapid and noticeable landscape features of permafrost thaw is the development of thermokarst lakes (Grosse et al., 2013). Thermokarst lakes form from the degradation of ice wedges in continuous permafrost areas, leaving standing water and unfrozen ground, called taliks, underneath the lake. The presence of thermokarst lakes, which have been forming in the Arctic since the Last Glacial Maximum, have been increasing and existing lakes have been expanding. Thermokarst lakes increase the amount of standing water that is present in the Arctic tundra. Standing water poses a challenge for tundra vegetation remote sensing. The tundra is studded with thermokarst lake depressions that form due to the freeze-thaw cycle of permafrost, and in the summer much of the tundra is covered with standing water. Water most strongly interferes with the retrieval of vegetation reflectance in the visible range (400 – 700 nm), but it can also cause a reduction across the entire spectrum. This can potentially influence vegetation signals retrieved from vegetation indices such as NDVI which use red reflectance (~650 nm although this varies by sensor), or PRI which uses green (~ 531 nm). Liquid water absorbs light in the NIR, reducing vegetation reflectance in that region, thus dampening vegetation signals in pixels with standing water (Lang et al., 2015). Remote sensing instruments with finer spatial resolution (< 30 m) can help to solve this problem by improving pixel purity.

The amount of vegetation cover varies significantly across the Arctic tundra due to differences in topography and soil properties such as nutrient content (Liu et al., 2017). Exposed bedrock and bare soil are common and bare soil can be intermixed with sparse vegetation cover. Soil and rock spectra vary depending on the type and color of the substrate and moisture content. Most dark colored soils are more strongly absorptive in the visible range than vegetation, but the vegetation signal is more strongly reflective in the NIR than soil. As with water, interference in the red and NIR can confound commonly used vegetation indices such as NDVI. Another complication is senescent or dry vegetation, which can have a spectral signal similar to bare soil (Liu et al., 2017). In the High Arctic, tundra vegetation can have a very brief growing season, so it is important that remote sensing measurements have short revisit times (daily) to capture phenological changes appropriately and tease apart vegetation from bare soil or litter.

Tundra fires have a sparse historical record, but recent data and model projections indicate that tundra fires will increase in frequency and severity under climate change (French et al., 2015). Fire has become a growing concern as a source of tundra change. Spectrally, burned vegetation reflectance is high in the shortwave NIR which can help distinguish it from green vegetation, but bare soil which is exposed during burning can interfere with vegetation retrieval (Boelman et al., 2011). Alternative vegetation indices have been proposed to assess burned vegetation areas, but full spectral data will help to tease apart burned areas from green vegetation.

3.6. Mixed Composition Observations

Although many tundra vegetation communities can often contain both vascular and non-vascular species, the combined spectral signature can be distinct enough to allow for separability

among communities. For example, (Davidson et al., 2016) successfully distinguished among eight different tundra vegetation communities including bryophyte-shrub, bryophyte-lichen, and tussock-shrub utilizing the Blue (450-510 nm), Red (640-692 nm) and Red Edge (705-745 nm) regions (Figure 5). Bratsch et al. (2016) distinguished among four tundra plant communities at Ivotuk, Alaska (particularly early in the growing season), using Blue, Red, and Near-Infrared bands. Both studies illustrate that it is possible to spectrally unmix Arctic plant communities, and that utilizing high spectral resolution data (1 nm) may help us to create spectral targets that can be teased apart from coarser spectral resolution datasets.

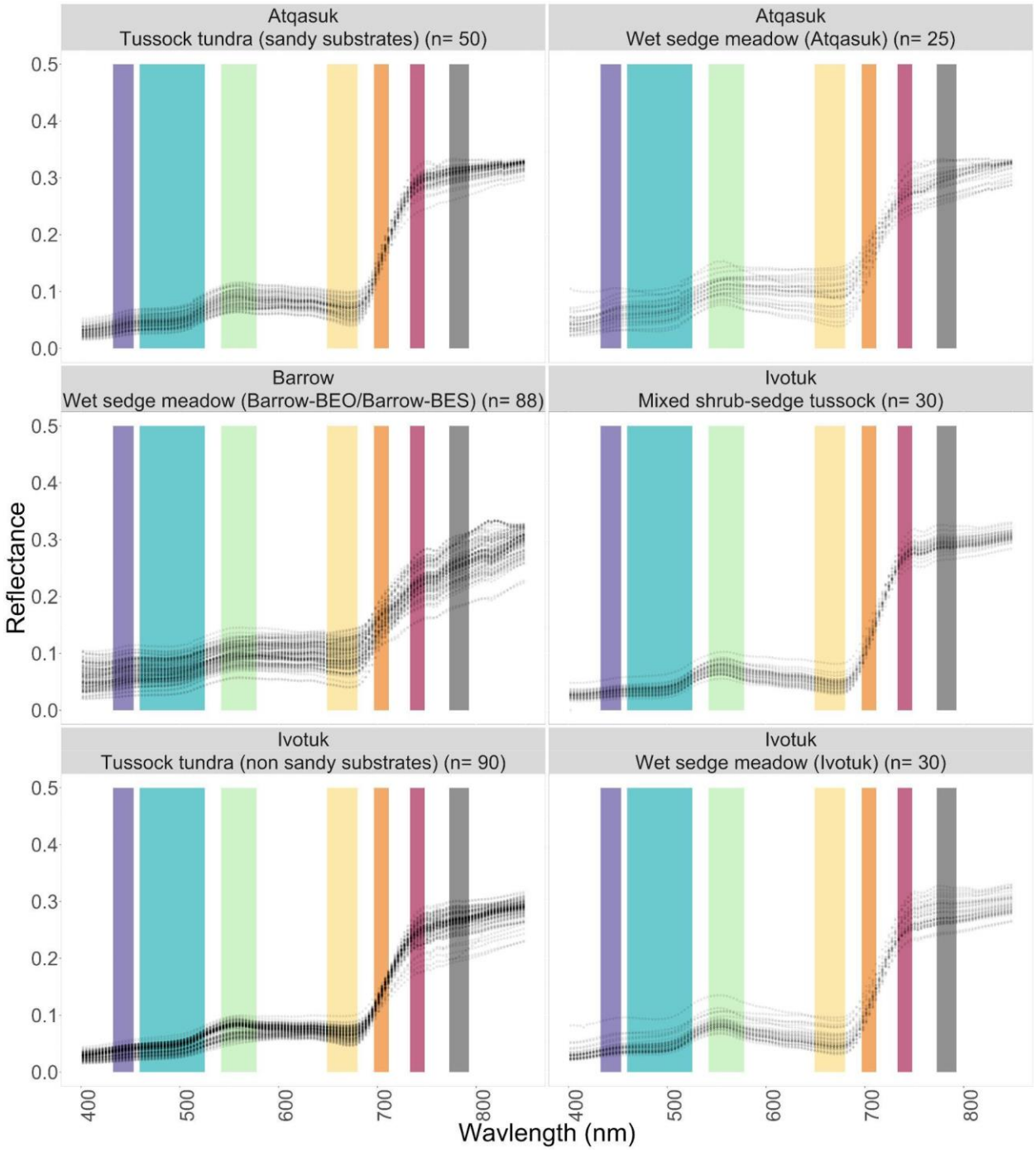

730

731 **Figure 5**. Spectral reflectance of mixed-composition pixels from representative tundra sites in
732 Alaska. Figure adapted from (Davidson et al., 2016). Sample size (n) is shown parenthetically.
733 Sentinel-2 bandpasses are indicated with colored vertical bars to illustrate the advantage of
734 imaging spectrometers with contiguous bands over multispectral instruments. Dots are opaque to
735 show the density of observations. Spectra were collected using a UniSpec DC Analysis System
736 (PP Systems, Amesbury, MA, USA) with a spatial resolution of 50 cm.

4. Uses of Spectroscopy for Tundra Studies

4.1. Long-term Vegetation Changes with NDVI

Long-term satellite data has revealed "greening" of Arctic tundra since the 1970s based on increases to NDVI derived from Landsat and AVHRR time-series data (Myers-Smith et al., 2020; Wang & Friedl, 2019). While tundra greening remains the most common trend across the Arctic, "browning", represented by a decreasing trend in NDVI values, has occurred in various regions and scales across the tundra (Myers-Smith et al., 2020). Greening and browning trends were one of the first indications that the Arctic tundra was being significantly impacted by climate change. Variations in greening/browning over different years have most commonly been attributed to climate warming (e.g., Berner et al., 2020; Bhatt et al., 2021; Cooper, 2014), herbivory by small mammals (Olofsson et al., 2012), and vegetation disturbance and subsequent recovery after extreme warming events (Bokhorst et al., 2012). However, there are significant limitations of the sensitivity of NDVI to high latitude ecosystem change (Huemmrich et al., 2021). For example, recent evidence suggests that some of these changes' impacts are fine-scale in nature (i.e., < 5-30 m), making many common remote sensing platforms impractical for studying these dynamics (Myers-Smith et al., 2020; Niittynen et al., 2020). Moving beyond greening and browning into the shifting landscape of numerous other metrics unlocked by IS, such as changes in land cover type and biophysical traits, will provide key insights into the magnitude and nature of high latitude ecosystem change.

From the outset, advanced IS data collections, such as from SBG, should be organized and calibrated to allow for future analysis of multi-year trends. In addition, improved land cover descriptions from SBG will enhance the interpretation of the existing NDVI trend analyses by establishing the capacity of different land cover types to respond to environmental change and

for that change to be reflected by observable changes in NDVI. Ground measurements collected over extended time series will improve our understanding of the nature of spectral reflectance change associated with measured land cover change and inform remote sensing needs.

4.2. Land Cover and Vegetation Classification

Surface reflectance data have long been used to classify and map vegetation types from landscape to global scales. Accurate data identifying the distribution of and changes to land cover types provide a significant opportunity for understanding Arctic environmental change. Improved mapping and classification of circumpolar land cover and its changes will be key to understanding the effects of global environmental change on Arctic ecosystems (Sections 4.2-4.4). Overcoming the challenges associated with mapping land cover at appropriate levels of thematic, spatial, and temporal detail will ultimately provide a significant advancement in our understanding of Arctic ecosystems.

Mapping Arctic vegetation types at high spatial resolution and with sufficient thematic detail has been challenging in part due to a relative sparsity of spectroscopic data. Global-scale land cover maps, such as the MODIS land cover product (Sulla-Menashe et al., 2019), are typically produced at a level of thematic detail that cannot distinguish between functionally distinct landforms (e.g., low- versus high-centered polygons) and vegetation types (e.g., low versus tall shrublands) present in Arctic tundra. Different arctic vegetation types are often combined into simpler, but less effective classes, or are represented by inappropriate classes (e.g., “grassland”) which do not reflect tundra ecosystem composition. The utility of land cover maps for tracking Arctic environmental change hinges on improving land cover classification, as subtle changes in

781 vegetation properties, such as increased shrub abundance, do not necessarily involve a transition
782 from one class to another within a mapped pixel.

783 Moving beyond land cover types and into the mapping of plant functional types or finer
784 taxonomic groups (e.g., family or genus) from spectra may be possible at continental scales if IS
785 data with large spatial coverage (> 1000 km^2 such as the ABoVE airborne campaigns (Section 2)
786 and SBG) are harnessed and developed. Acquiring and applying more detailed spectroscopic
787 data for Arctic vegetation types will enable mapping with improved thematic detail, particularly
788 if they are analyzed in tandem with ancillary high spatial resolution datasets that capture
789 important environmental covariates such as topography (e.g., ArcticDEM) and edaphic
790 characteristics (e.g., seasonal inundation, snow depth and hardness, active layer thickness, depth
791 to water). Few studies have yet applied detailed IS data to map Arctic vegetation types (Smith et
792 al., 2021; Thomson et al., 2021), but an increase in available imagery may enable future work in
793 this area.

794 Land cover maps with classifications designed for Arctic vegetation types are typically
795 limited in spatial or temporal range (Chasmer et al., 2014; Greaves et al., 2019), precluding
796 comprehensive study of Arctic vegetation dynamics, or are coarse in spatial or temporal
797 resolution (e.g., gridded 1 km CAVM) (Raynolds et al., 2019), precluding accurate
798 characterization of the high level of spatial heterogeneity and temporal variability in Arctic
799 vegetation. Bartsch et al. (2016) suggested that a 30 m spatial grain, which is the proposed
800 spatial resolution for SBG, is sufficient for capturing many of the dynamics of Arctic land cover.
801 However, depending on whether species-level or functional type-level maps are being generated,
802 even higher spatial resolution (e.g., 3 m from Planet) may be insufficient to distinguish Arctic
803 vegetation except at broad thematic levels (e.g., trees vs. shrub vs. water). Therefore, the use and

804 further development of advanced subpixel mixture analysis will enable high accuracy vegetation
805 classifications with reasonable instrument spatial resolution and broad spatial coverage
806 (Thomson et al., 2021). Tapping the information content of higher spatial resolution data (e.g.,
807 Section 2) will be essential to preparing the algorithms and analysis pipelines to utilize a
808 spaceborne imaging spectrometer such as SBG that has a finer spectral resolution occurring at an
809 intermediate spatial resolution to map Arctic vegetation (Section 5).

810 Another key limitation to mapping vegetation in Arctic tundra is the lack of high-quality,
811 georeferenced training data. Existing observations are scattered across numerous countries, land
812 management agencies, and historical datasets. Disparate datasets often do not capture similar
813 levels of detail, and thus can be challenging to integrate. Land cover maps, and the algorithms
814 and data that go into producing them, are only as credible as the underlying training data.
815 Typically, land cover maps are trained on datasets of land cover type that are produced by visual
816 interpretation of very high spatial resolution imagery (e.g., using Google Earth), but the
817 availability of suitable (midsummer) imagery is extremely limited in the Arctic tundra (Section
818 1). Field data provide the most reliable source of georeferenced Arctic ground verification, but
819 they are inherently limited in scope and are spatially biased towards areas with a long history of
820 research (e.g., northern Alaska's Dalton Highway corridor). Airborne data (including UAS
821 observations) can bridge the scaling from field data to spatially extensive gridded datasets
822 (Assmann et al., 2020). This scaling will ultimately enable training of machine learning
823 algorithms to effectively map Arctic vegetation at continental scales.

824 Finally, the unique seasonal characteristics of the Arctic impose additional challenges on
825 mapping tundra vegetation at scale. Phenological differences can help to separate co-occurring
826 and spectrally similar plant functional types (Macander et al., 2017), but the phenology itself is

highly variable through space and time since it is sensitive to moisture status and interannual variability in meteorologic conditions (Sections 4.4 and 4.5). Land cover mapping algorithms may misinterpret spectral changes caused by interannual variation as real land cover change. The brief snow-free season in the Arctic tundra may inhibit sufficient characterization of phenology-driven spectral changes, which further reduces our ability to identify spurious change detection. A sufficiently large and representative training dataset, as described above, will help prevent vegetation mapping algorithms from misclassifying changes in moisture status and phenology with changes in land cover in the Arctic Tundra.

4.3. Retrieval of Biophysical Properties and Plant Traits

The strong connection between IS and the biophysical properties of plant leaves and canopies makes it possible to retrieve a host of important vegetation properties with spectroscopy (Serbin & Townsend, 2020). Particularly, the mapping of plant functional traits, i.e., the morphological, biochemical, phenological, and physiological attributes of leaves and canopies (Violle et al., 2007), has been a priority and key focal area of study (Asner et al., 2015; Asner & Martin, 2008; Cawse-Nicholson et al., 2021; Singh et al., 2015; Z. Wang et al., 2019, 2020) . These functional traits, which are closely related to vegetation establishment, growth, and functioning, are key to understanding vegetation responses to climate change, as well as process modeling of terrestrial ecosystems (Gamon et al., 2019; Myers-Smith et al., 2019; Xu & Trugman, 2021; Zakharova et al., 2019). For example, traits that describe leaf photosynthetic capacity (e.g., foliar pigments, nitrogen, and V_{cmax}), biogeochemistry (e.g., ligno-cellulose, carbon, and macronutrients), and water cycling (e.g., stomatal conductance) are important to characterize ecosystem carbon, water, and energy cycling and response to climate change (Chapin, 2003; Myers-Smith et al., 2019; Ollinger & Smith, 2005; Rogers et al., 2017; Tang et al., 2018; Woodward & Diament, 1991) .

Similarly, traits related to vegetation structure, such as leaf area and canopy height, are important for determining ecosystem energy partitioning (e.g., through surface albedo and temperature), as well as surface-atmosphere interactions (Aalto et al., 2018) that feedback to the global climate system (Zhang et al., 2018).

In the Arctic, plant functional traits vary remarkably within and across plant species and over space and time, controlled by the complex, fine-scale gradients (0.1-10 m) in climate, topography, water, and nutrients (Andresen & Lougheed, 2021; Bjorkman et al., 2018; Black et al., 2021; Chen et al., 2020; Thomas et al., 2020). In particular, traits that confer differing competitive advantages, such as those related to plant size and resource economics (e.g., leaf area, seed mass, height, LMA, N, LDMC) (Thomas et al., 2020), are highly sensitive to changes in micro-environments, making them difficult to characterize with traditional field surveys (Metcalfe et al., 2018; Schimel et al., 2015). In addition, the photosynthetic capacity (V_{cmax} and J_{max}) and response to environmental conditions of Arctic plants are significantly different from the current assumptions in the process models used to forecast Arctic change (Rogers et al., 2017).

Non-vascular plants which dominate large areas of the Arctic, have very different biochemical attributes and possess morphologies that are not yet easily measured (Sections 3.2-3.3) (Holt & Nelson, 2021). Water content varies in non-vascular plants based almost entirely on environmental conditions since they do not actively conduct water, which greatly influences their spectral signatures (Figure 4). Variable water content in the non-vascular ground layer visible to remote sensing instruments presents a primary challenge and significant opportunity to understand ecosystem function. Methods using a combination of VNIR, SWIR, and MIR show promise for addressing water content in non-vascular plants (Granlund et al., 2018; Neta et al.,

873 2010). Testing these estimations of water content at large spatial scales (> 1 E4 km^2) remains a
874 challenge. Most traits in non-vascular plants exhibit different spectral responses from those of
875 vascular plants (Cornelissen et al., 2007), precluding direct use of existing trait retrieval
876 approaches developed for vascular plants. Recent work by Thomson et al. (2021) shows that
877 chemometric estimation in non-vascular plants using remote sensing is possible but there are
878 only a few species studied over a small area (< 1000 km^2). Collectively these challenges have
879 created significant uncertainties in our understanding and modeling of Arctic ecosystems (Fisher
880 et al., 2018; Metcalfe et al., 2018; Myers-Smith et al., 2019). Developing algorithms to estimate
881 properties of non-vascular plants using spectra and remote sensing will enable more accurate
882 quantification of plant functional traits.

883 IS can provide a tool to spatially map a variety of plant functional traits across scales (e.g.,
884 from watershed to biome) which has been demonstrated in many other biomes (e.g., Asner &
885 Martin, 2008; Martin et al., 2008; Singh et al., 2015; Z. Wang et al., 2019, 2020). The launch of
886 SBG and other IS missions (e.g., EnMAP) will provide important data to further enable
887 spatiotemporal mapping of traits across the broader Arctic tundra biome (Cawse-Nicholson et al.,
888 2021) . Simultaneously, spectral data from aircraft (e.g., Miller et al., 2019) and low-altitude,
889 near-surface platforms, including automated trams (Gamon et al., 2006; Goswami et al., 2011;
890 Healey et al., 2014), tower-mounted instruments (e.g., Drolet et al., 2014; Hilker et al., 2011),
891 and unoccupied aerial systems (Assmann et al., 2020; Cunliffe et al., 2021; Shiklomanov et al.,
892 2019; Yang et al., 2020), have increased in northern high latitudes. These diverse spectral
893 platforms are likely to revolutionize our means for collecting trait information, which could
894 usher a new paradigm in our understanding and modeling of Arctic vegetation dynamics. For
895 example, using traits derived at watershed and larger scales, the spatial variation in traits across

plant species, plant functional types (PFTs), communities, and even ecosystems can be easily characterized (Figure 6). The drivers of spatial variation in plant traits can also be investigated in combination with other core remote sensing datasets, such as topography, climate, soil properties, and vegetation maps, which is a key to understanding plant responses to climate change (Durán et al., 2019). In addition, as a critical uncertainty in process models (Rogers et al., 2017), the spatial information on plant traits and biophysical properties inferred from IS could be directly integrated with models to inform and improve predictions (Fer et al., 2018; Shiklomanov et al., 2021), thereby reducing current predictive uncertainties (Dietze et al., 2014).

The high spatial heterogeneity in vegetation composition, structure, and abiotic environments (Section 3) pose a challenge to retrieve plant traits using spectroscopy in the Arctic (Thomson et al., 2021; Yang et al., 2021). Traditional radiative transfer model-based retrieval assumes the underlying vegetation layer to be homogeneous (Jacquemoud et al., 2009), which is not met in tundra landscapes. Empirical modeling that builds statistical relationships between field trait observations and remote sensing spectra using machining learning or latent variable techniques is a powerful alternative (Curran et al., 1997; Singh et al., 2015; Z. Wang et al., 2020; Wold et al., 2001). However, to construct an empirical model, a plot-to-pixel connection is required. This requirement can be easily met in forest or managed ecosystems where a single tree can occupy one or multiple image pixels or a vegetation layer is homogenous across relatively large areas. The Arctic poses challenges to plot-to-pixel connections given the high level of species mixing in imagery pixels of > 5 m resolution, which, combined with the remote and meteorologically harsh environment, restricts the collection of quantitative plot observations to develop trait models.

Unoccupied Aircraft Systems (UAS) remote sensing collects spectral data at a very high spatial resolution and has shown great promise to serve as an intermediate data source to connect ground and high-altitude platforms (Thomson et al., 2021). In addition to the high spatial heterogeneity, the common presence of non-vegetated surfaces (e.g., water, soil, rocks, and litter) and their highly variable spectral characteristics (Section 3.5), present additional challenges to the mapping of traits. Typically, non-vegetated surfaces can be excluded over the course of trait model development and application in low-latitude ecosystems (e.g., Wang et al., 2019), but non-vegetated surfaces are highly mixed with vegetation surfaces in the Arctic, which must be accounted for in trait model development. Lastly, the short growing season and harsh environment means that vegetation spectra and traits can change rapidly during the growing season (Section 4.4). Therefore, trait models built from data collected at a certain time of year may only be applicable to a narrow temporal window (e.g., < 1 month), as compared to low-latitude ecosystems where vegetation growth peaks can persist for several months. SBG and other time-series spectral platforms (e.g., PACE, CHIME, DESIS, EnMAP) hold great potential to address this issue by facilitating the development of time-series models that capture seasonal trait dynamics.

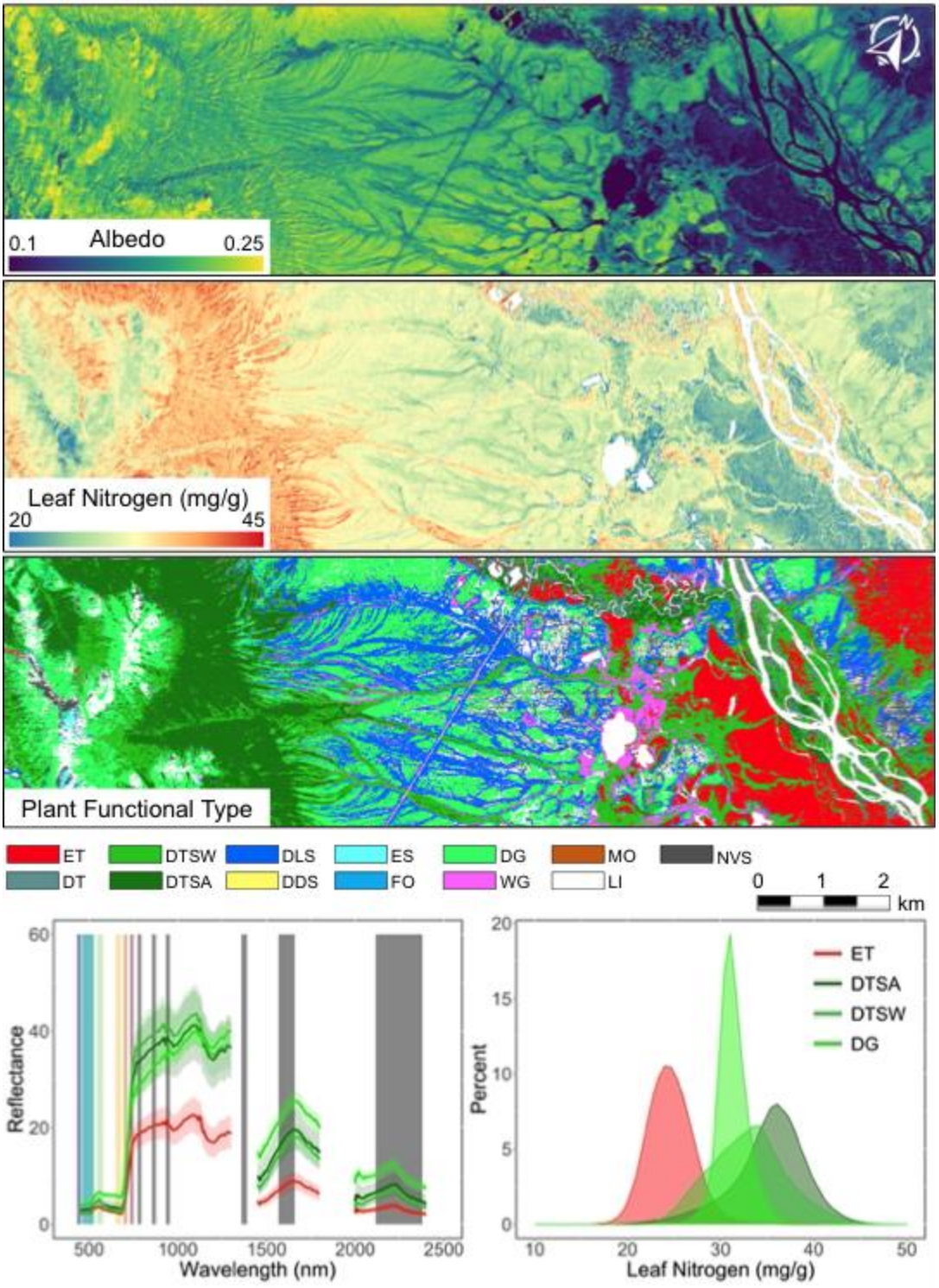

934

935 **Figure 6.** Example full shortwave (i.e., 350-2500 nm) albedo and leaf nitrogen map, spectral
936 variation and trait distribution across main plant functional types or plant community types (Serbin
937 et al., unpublished). Observations were collected from AVIRIS-NG at the Seward Peninsula, AK.
938 The PFT spectra shown in the bottom-left panel are derived from AVIRIS-NG pixels that are at
939 least 85% dominated by the (PFTs). Sentinel-2 bandpasses are indicated with colored vertical bars

to illustrate the advantage of imaging spectrometers with contiguous bands over multispectral instruments. Evergreen tree (ET), deciduous tree (DT), deciduous tall shrub-alder (DTSA), deciduous tall shrub-willow (DTSW), deciduous low shrub (DLS), deciduous dwarf shrub (DDS), evergreen shrub (ES), forb (FO), dry graminoid (DG), wet graminoid (WG), moss (MO), and lichen (LI).

4.4. Phenology

Phenological change in the tundra is characterized by rapid transition seasons with volatile weather patterns. Snow cover over the winter months and along the transition seasons complicates our ability to use remote sensing metrics to detect such phenological change. Vegetation indices that track both chlorophyll content (e.g., NDVI, NIRv, and EVI) as well as photosynthetic capacity (e.g., PRI and CCI) are all sensitive to the presence of snow cover and emergent senescent vegetation (Gamon et al., 2013; Luus et al., 2017; Pierrat et al., 2021) (Figure 7). Further, photosynthesis of Arctic tundra vegetation may occur under snow cover (Parazoo et al., 2018; Starr & Oberbauer, 2003), thereby severely hindering the utility of spectroscopy for even detecting primary productivity throughout the year. Reliance on these measures without appropriate snow cover correction significantly inhibits their utility to determine phenological change over winter and transition seasons. For many tundra species, especially lichens, bryophytes, and evergreen shrubs and trees exhibiting limited intra-annual biomass production, changes in structural indices such as NDVI, NIRv, and EVI may better capture changes in snow on/off periods than actual changes in biomass (Figure 7) (Gamon et al., 2013; Luus et al., 2017; Pierrat et al., 2021). Cold temperatures and the lack of liquid water can force dormancy and limit photosynthesis, but if the vegetation remains green, changes in NDVI may be nominal. Tundra species have been shown to acclimatize to winter conditions by increasing the size of their pool of xanthophyll cycle pigments and by maintaining that pool

largely as antheraxanthin and zeaxanthin (Verhoeven, 2014), which manifests as an increase in total carotenoid pigments, and can be captured by the CCI (Gamon et al., 2016; Wong et al., 2020). In evergreen needleleaf trees, strong seasonal variation in photoprotective pigments can be detected via PRI and CCI - attuned to variation in xanthophyll and bulk carotenoid pigments, respectively (et al., 2016; Wong & Gamon, 2015b, 2015a). Strong linkages between sensitivity of cessation of radial stem growth in TTE spruce trees to end-of-season meteorology is also detectable by changes in PRI (Eitel et al., 2019, 2020). Similar investigations of PRI/CCI-growth and photosynthesis relationships on (non-tree) tundra vegetation would help advance understanding of Arctic tundra phenology. In addition, plant pigment composition serves as an important indicator of the timing of autumn entry into this seasonally downregulated (*i.e.*, dormant) state (Figure 7). Hence, phenological analysis of tundra vegetation requires integration of multiple spectral metrics, preferably including narrowband measurements related to photoprotective pigment variation, to isolate seasonal change in plant structural and functional

dynamics from confounding variation in snow cover.

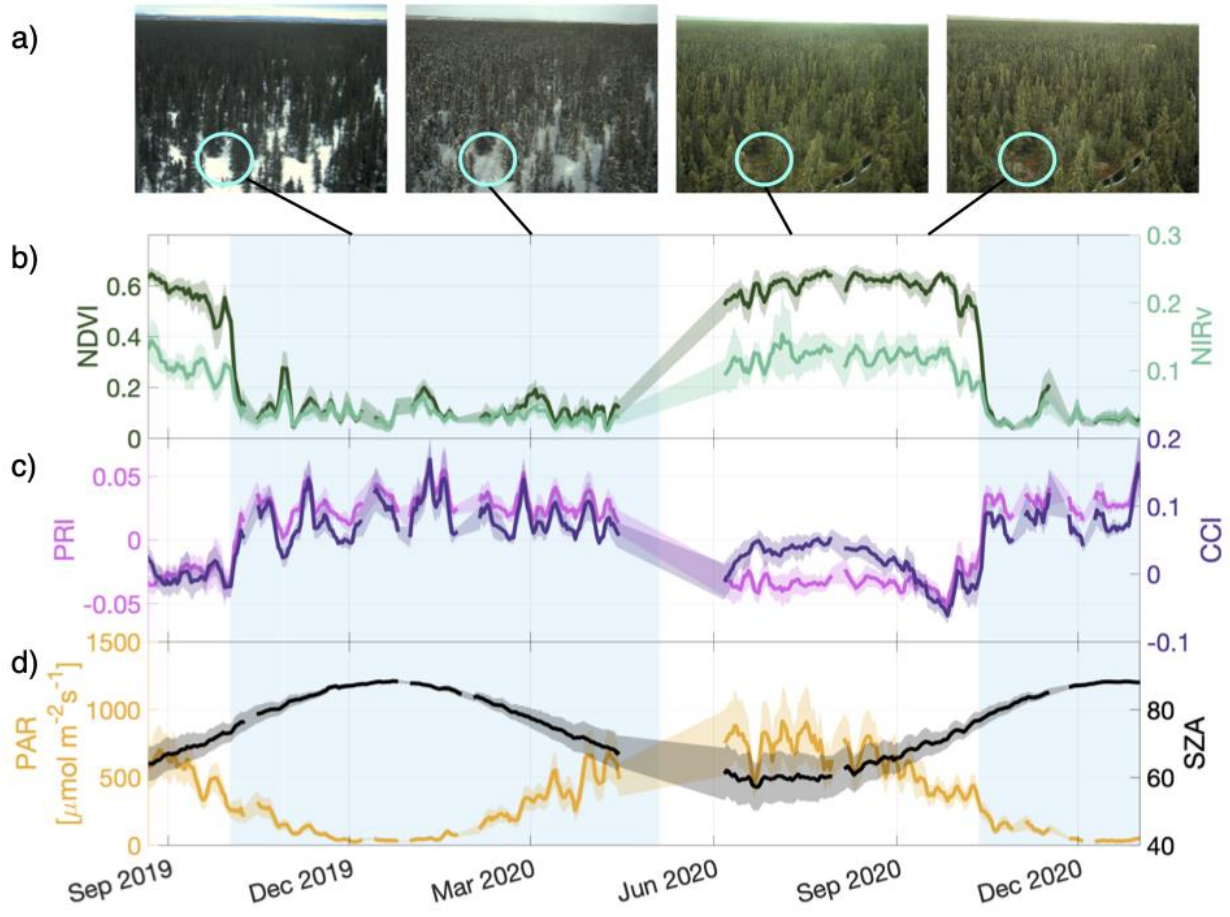

Figure 7. a) Shows phenocam images from different points during the year with varying degrees of snow cover on understory/tundra vegetation at NEON Delta Junction, AK. b)-c) Shows commonly used vegetation indices (NDVI, NIRv, PRI, and CCI) measured from a tower-based spectrometer system PhotoSpec (Grossmann et al., 2018) observing three understory tundra targets at a 30-minute resolution. d) Shows daily average PAR and SZA. For b)-d), plotted is the 5-day moving mean of the measured quantity. Shaded error bars indicate the standard deviation of diurnal variability. Shaded blue regions indicate the presence of snowfall on the understory as determined visually from phenocam images.

Many spaceborne instruments are temporally incompatible with the rapid phenological progression of tundra within a compressed growing season. Historically, analyses of seasonal change across the Arctic may leverage time series observations by the Landsat missions.

992 However, the 16-day revisit frequency precludes accurate detection of timing of important events
993 to quantify interannual variability in phenology. The similar temporal resolution (14-day revisit)
994 proposed for SBG may yield similar challenges for phenology applications. Furthermore, due to
995 the prevalence of cloud cover, infrequent observations reduce the opportunity for clear-sky
996 imaging resulting in seasonally sparse or irregular observations. Both these issues are made
997 apparent by tower-based observations (Figure 7), which enable continuous or high frequency
998 observations but lack the spatial coverage of spaceborne observations. Tower-based observations
999 in the boreal forest showed a 29 day difference in the timing of the springtime onset of
1000 photosynthesis between evergreen and deciduous tree species (Pierrat et al., 2021). Such
1001 temporal asynchrony - including among evergreen and deciduous tundra plants - may not be
1002 adequately captured by spatially and temporally coarse resolution spaceborne data. Thus, tower-
1003 based observations will play an integral role in understanding Arctic phenological change. Co-
1004 incident UAS observations can help bridge the spatiotemporal gap through repeated
1005 measurements at a lower temporal resolution than tower-based but at a much higher spatial
1006 range.

1007 **4.5. Diurnal variation**

1008 The primary intrinsic mechanisms driving diurnal changes in spectral reflectance are related
1009 to plant pigment composition, which regulate the efficiencies of photochemistry through dynamic
1010 changes in photoprotective pigment pools (xanthophylls, lutein) via sustained and rapidly
1011 reversible non-photochemical quenching (Adams et al., 2004), and hydration status for non-
1012 vascular vegetation. Dynamics among a cycling group of carotenoids, violaxanthin,
1013 antheraxanthin and zeaxanthin (V, A, and Z, respectively), known as the xanthophyll cycle, are
1014 especially informative in this regard (Demmig-Adams et al., 1996). During the photosynthetically

active season, the state of the xanthophyll cycle responds to diurnal variation in incoming light via enzymatically regulated conversions between Z + A and V. These dynamics are often captured using spectral indices sensitive to changes at 531 nm (the photochemical reflectance index, PRI, (Gamon et al., 1992)). However, most other vegetation spectral changes are not associated with diurnal physiological dynamics; hence, these spectral indices (i.e., NDVI, NIRv, and CCI) can remain relatively invariant (Figure 8) with the exception of changes in moisture status for non-vascular vegetation (Figure 4). Most spectral changes in the VIS-SWIR range throughout the course of the day are associated with changes in viewing-illumination geometries, as illustrated in subplots of NDVI, NIRv, CCI in Figure 8.

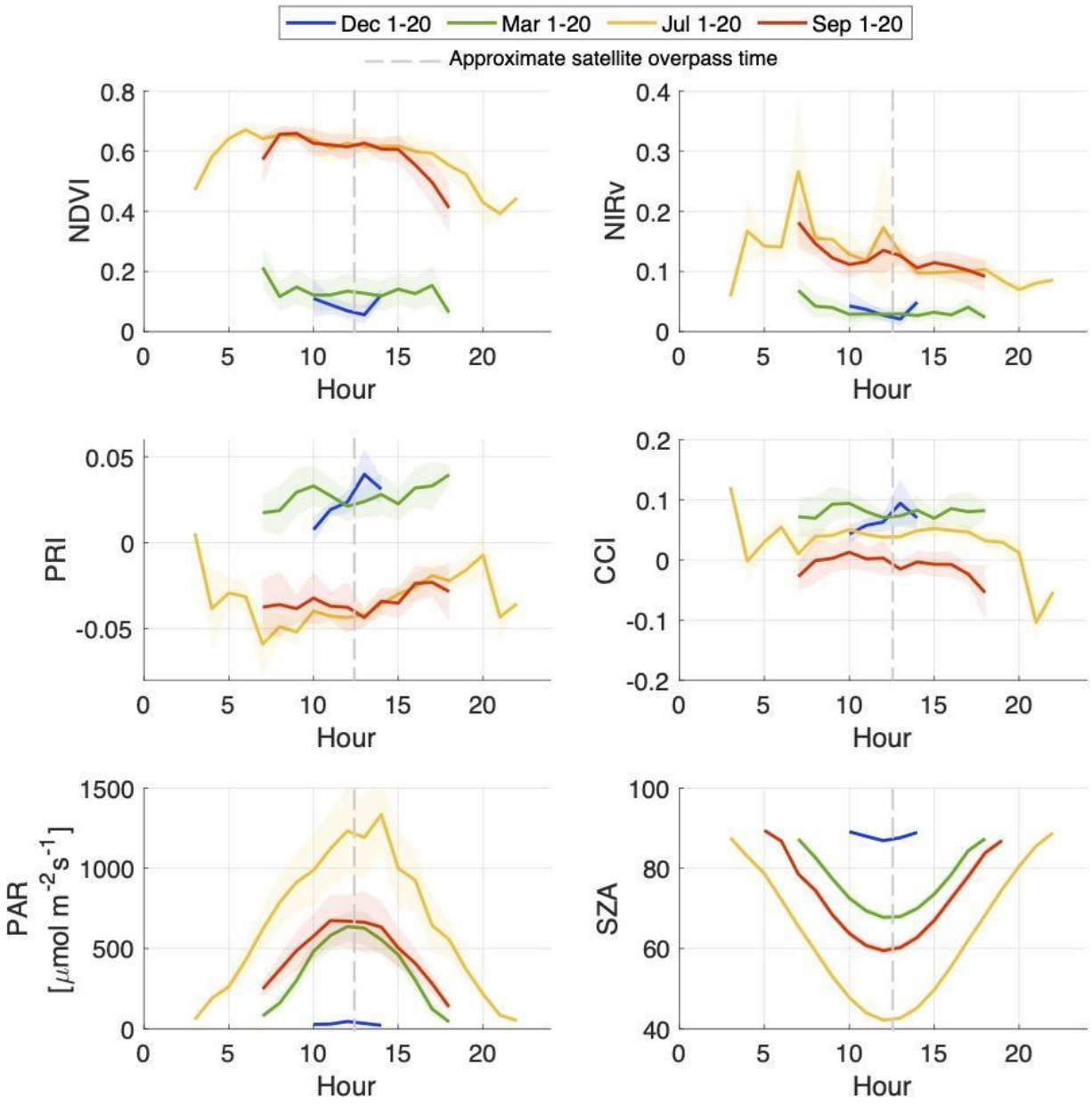

1024

1025 **Figure 8**. Diurnal cycles of commonly used vegetation indices (NDVI, NIRv, PRI, CCI), PAR,
1026 and SZA collected from PhotoSpec at NEON Delta Junction, AK for three vegetated understory
1027 targets. Diurnal cycles are the average cycle over the 20 day period indicated and shaded error
1028 bars are the standard deviation of measured quantities over the 20 day period.

1029

1030 The interaction of orbital mechanics with diurnal and seasonal variation in vegetation indices

1031 results in possible bias due to overpass timing of spaceborne instruments (Xiao et al., 2021). As

shown in Figure 8, some indices are diurnally invariant (e.g., NDVI, NIRv, and CCI) whereas PRI is not. Consistent observation in the morning versus afternoon may result in discrepancies in comparing observations from multiple instruments and platforms. Relying exclusively on observations from either morning or afternoon may obscure important diurnal processes at work that govern plant productivity (see discussion of xanthophyll cycle dynamics, above). On a seasonal basis, the extended diurnal photoperiod experienced by high latitudes provides an opportunity for higher frequency observation (i.e., multiple per day) of vegetation spectra by spaceborne instruments during the peak season; however, this potential advantage of deploying sensors that can collect multiple daily observations rapidly diminishes in the shoulder seasons and winter when photoperiod is abbreviated or non-existent (i.e., polar winter, Figure 8). Therefore, interpreting time series vegetation indices from Arctic tundra requires careful accounting for overpass timing, photoperiod, and all associated responses to diurnal physiology and viewing/ illumination geometry.

5. Recommendations

In ecosystems characterized by low accessibility and challenging terrain, including the Arctic tundra, remote sensing observations provide the only practical approach for observing, monitoring, and quantifying changes in vegetation structure, function, and distribution. However, to make the best use of these data and provide useful information for ecological research and specifically process modeling requires converting the remotely sensed observations (e.g., surface radiance or reflectance) to derived biophysical or functional quantities of interest (e.g., leaf area index, leaf functional traits). A range of approaches have been used to convert spectroscopic

measurements to plant properties (Cawse-Nicholson et al., 2021; Gamon et al., 2019; Serbin & Townsend, 2020). However, the distinctive characteristics of the Arctic as described above requires different approaches that incorporate effective scaling to allow for mapping Arctic vegetation composition and function; developing these approaches remains a critical need and challenge.

To address this challenge, we recommend that a multi-scale approach (Table 2), including a mix of observations from laboratory, field, and novel platform studies (e.g., UAS, tower-mounted, sensor network including SpecNet) is used in coordination with satellite overpasses when possible. These observations must then be assessed cohesively, together with appropriate statistical and radiative transfer modeling (Figure 9, Table 2). Leaf-scale and controlled laboratory studies are often used to identify fundamental, underlying drivers of variation in leaf optical properties to aid in the development of algorithms for estimating leaf functional traits or evaluating leaf stress (e.g., Féret et al., 2011; Gamon et al., 1997; Hunt & Rock, 1989). However, such work has historically been limited in the Arctic in comparison with other ecosystems, suggesting that considerable uncertainty will remain through efforts to tie spectral observations to vegetation function. To efficiently address this issue, future spectroscopy campaigns should engage with laboratory and field studies to determine where multi-scale observations could be established.

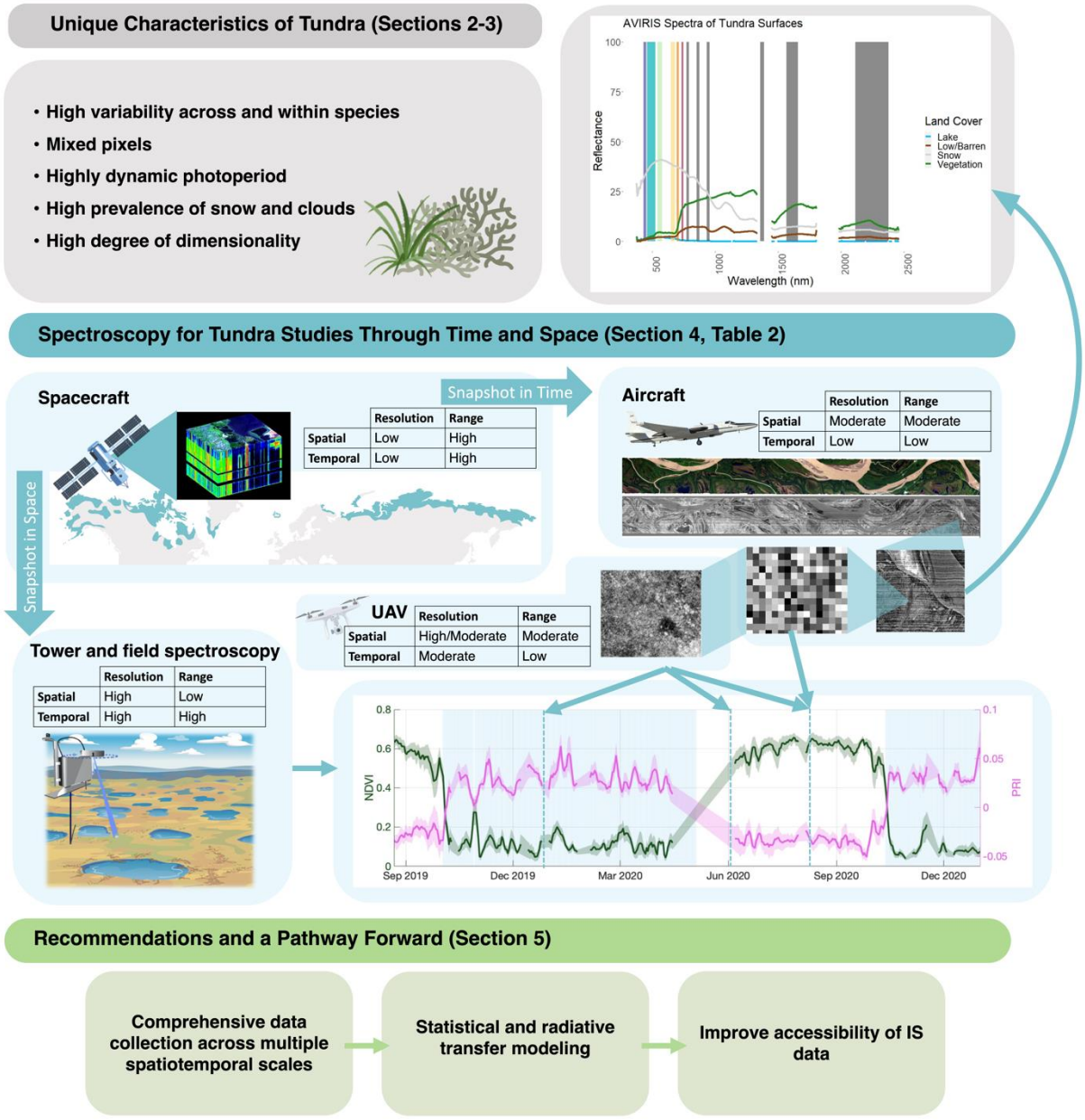

Figure 9. Framework for advancing understanding of Arctic tundra ecosystem properties and dynamics through spectroscopy.

1079 **Table 2**. Example recommended spectroscopic observations across spatial scales that, coupled
1080 with spaceborne missions like SBG, would improve understanding of Arctic tundra ecology.

1081

Measurement type	Spatial scale	Temporal Scale	Purpose	Methods	Example Citations
Laboratory or leaf-level	<< 1 m	Snapshot	Variation in leaf-level optical properties; spectral response to stress (e.g., drydown); development of leaf-scale functional trait models	Collection of leaf and canopy spectra in controlled, manipulation environments and in situ; leaf spectroscopy; collection of leaf endmember spectra	(Hunt & Rock, 1989; Serbin et al., 2019; Stasinski et al., 2021)
Field spectroscopy	<1 m - 10 m Canopy	Snapshot	Variation in spectral profiles by species at different scales; developing scaling approaches	Near-surface, non-contact measurement of plant canopy reflectance	(Davidson et al., 2016; Karl Fred Huemmrich et al., 2013)
Tower or automated tram	100s of m Canopy - Landscape	Continuous (hourly) over seasons	Diurnal and seasonal variation; variation between species; developing scaling approaches	Repeated manual or automated measurement of plant canopy reflectance	(Hilker et al., 2011; Pierrat et al., 2021)
UAS	0.2 - 1 m Landscape	Snapshots	Fine-scale spatial information at landscape to watershed scales; scaling; seasonal variation	Collection of surface reflectance and other composition and structural information from unoccupied platforms	(Thomson et al., 2021; Yang et al., 2021)
Piloted aircraft	0.5 - 5 m Landscap	Snapshots every	Regional mapping and	Imaging spectroscopy	(Maguire et al., 2021;

	e - regional	few years	intermediate scale of observation		Singh et al., 2015)
Spacecraft	10 m - 8 km Regional - continental	Repeating daily - weekly	Regional to continental-scale mapping, monitoring of coarse spatial resolution phenological change	Imaging spectroscopy, change detection and time series analysis	(Puletti et al., 2016; J. A. Wang et al., 2020)

Given the strong seasonality of Arctic vegetation (see Section 4.4), additional consideration of the timescale of measurement and underlying phenomena are critical to mapping efforts. Coupled observations across spatial scales that can be conducted with high observation frequency across seasons will help resolve this challenge (Table 2). Further, both seasonal and interannual evaluations of change in the Arctic tundra must consider the constraints of winter in terms of both sampling design and physiological effects. The rapid seasonal progression (as discussed in Section 4.4) imposes tremendous challenges for benchmarking the onset of seasonal photosynthetic activity and tissue growth, quantifying sensitivity to shoulder season stress, and detecting legacy effects on productivity in subsequent seasons. In particular, the strong seasonality of photoprotective pigments in evergreens (see Section 3.4 and 4.4), which complicate interpretation of spectral reflectance, requires further research across the Arctic tundra domain to improve parameterization of models of primary production. Additionally, deciduous shrub species exhibit strong autumn leaf coloration with photoprotective pigments present (and chlorophyll content declining) during leaf senescence that may facilitate remotely sensed quantification of species cover values. For example the red autumn leaves of birch continue to actively photosynthesize even though chlorophyll pigments may be less evident by

traditional greeness-based remote sensing (Patankar et al., 2013). Spectroscopy is well suited to address these challenges and could likely help disentangle the timing of vegetation responses among plant functional types.

The use of optical remote sensing information over large regions (i.e., across continents) and through time (i.e., multiple decades) has increased considerably in recent years (Ustin & Middleton, 2021). This includes IS data in the Arctic (e.g., (Langford et al., 2019)), given the increased availability of these datasets (Miller et al., 2019). However, new approaches for access, use, and analysis of large IS datasets will be needed given the growing volume of remote sensing observations across scales. For example, fusing high volume data from novel UAS and ground-based platforms and expanded use of datasets across scenes and locations will greatly increase the overall volume of data for any given project. Seasonal weather conditions and sun-sensor geometry changes in the Arctic mean that a considerable fraction of data may have variable data quality over scenes or across scenes in a study area. Similarly, current methods for retrieval of IS data require manual search, collection and combining of data across different locations by end-users. To ease and expand use of IS data for Arctic researchers, it is recommended that data systems provide analysis-ready (e.g., geo-rectified and consistent atmospheric correction) and cloud-optimized data storage formats (e.g., cloud-optimized GeoTIFF). In addition, files should be accessible on storage buckets (i.e., basic container that stores bulk data, usually used for organizing combinations of similar datasets, e.g., S3 or Google cloud bucket) through cloud-based tools to facilitate rapid search, filter, and extraction of data across specific locations, regions and scenes. Similarly, it is recommended that cloud-based tools facilitate basic analyses, data transformation, subsetting, and application of mapping algorithms without downloading large volumes of IS datasets but instead the final derived products or results of the cloud pre-

processing. For example, this could be facilitated through the use of a cloud storage location within Google Earth Engine (GEE) or GEE within the Python or R environments. By moving IS data access to the cloud would also facilitate easy combination with other remote sensing data or even multiscale observations, including UAS data. This would also reduce the data latency from collection to community use and allow more users to facilitate discovery of novel and important patterns in phenomena in the Arctic biome.

We described important attributes of tundra ecosystems that impose challenges for conducting spectroscopy, including plant functional type and pixel-composition characteristics, intrinsic dimensionality, and capacity for land cover classification, change detection, time series observations, and characterizing biophysical properties. Future spectroscopy missions such as SBG would be well-advised to consider the challenges of complex biomes such as the Arctic tundra during mission development and especially for data product generation. To address these challenges, an optimized mixture of narrow and broad bands should be considered for SBG to accurately characterize Arctic vegetation.

Acknowledgements

PRN and MJM were supported by NASA Arctic Boreal Vulnerability Experiment (ABoVE) Grant 80NSSC19M0112. AJM was supported by an appointment to the NASA Postdoctoral Program at the Jet Propulsion Laboratory, administered by Universities Space Research Association under contract with NASA. ZP was supported by the National Science Foundation (NSF) Graduate Research Fellowship under Grant No. DGE-1650604 and DGE-2034835. Any opinion, findings, and conclusions or recommendations expressed in this material are those of the authors(s) and do not necessarily reflect the views of the NSF. ELO and TSM were supported

by NASA ABoVE project 80NSSC19M0129. DY and SS were supported by the Next-Generation Ecosystem Experiment in the Arctic (NGEE Arctic) project that is supported by the Office of Biological and Environmental Research in the United States Department of Energy, Office of Science, and through the Department of Energy contract No. DE-SC0012704 to Brookhaven National Laboratory, and SS was also partially supported by the NASA Surface Biology and Geology (SBG) mission study (under contract #NNG20OB24A). GVF was partially supported by NASA ABoVE Grant NNH16CP09C. SFO and SU were partially supported by NSF Office of Polar Programs award number 1836898. SVZ, PKE, and KFH were partially supported by NASA ABoVE grant NNX17AC58A, and SVZ was also partially supported by NSF ITEX-AON 1836861. MV was partially supported by NOAA NA16SEC4810008. AVIRIS-NG data was supported by the National Aeronautics and Space Administration, Earth Science Division, and acquired by the NASA ABoVE project. The data shown in Figure 5 were collected under a project funded by the OPP of the NSF awarded to Donatella Zona (award number 1204263) with additional logistical support funded by the NSF OPP, and Carbon in Arctic Reservoirs Vulnerability Experiment (CARVE), an Earth Ventures (EV-1) investigation, under contract with NASA. A portion of this research was carried out at the Jet Propulsion Laboratory, California Institute of Technology, under a contract with NASA (80NM0018D0004).

Data Availability Statements

Orthorectified radiances in Figure 2 from AVIRIS-NG's ABoVE campaign acquisitions are available with documentation from the ORNL DAAC (https://doi.org/10.3334/ORNLDAAC/1569). They were analyzed with the ISOFIT atmospheric correction codebase (https://github.com/isofit/isofit). This software is also available via the DOI

https://doi.org/10.5281/zenodo.4614338). Data for Figure 2 are cited in the text with the references below:

AVIRIS-NG data citation:

Miller, C.E., R.O. Green, D.R. Thompson, A.K. Thorpe, M. Eastwood, I.B. Mccubbin, W. Olson-duvall, M. Bernas, C.M. Sarture, S. Nolte, L.M. Rios, M.A. Hernandez, B.D. Bue, and S.R. Lundeen. 2019. ABoVE: Hyperspectral Imagery from AVIRIS-NG, Alaskan and Canadian Arctic, 2017-2019. ORNL DAAC, Oak Ridge, Tennessee, USA. https://doi.org/10.3334/ORNLDAAC/1569

ISOFIT citation:

Thompson, David R., Vijay Natraj, Robert O. Green, Mark C. Helmlinger, Bo-Cai Gao, and Michael L. Eastwood. "Optimal estimation for imaging spectrometer atmospheric correction." Remote Sensing of Environment 216 (2018): 355-373. https://doi.org/10.1016/j.rse.2018.07.003

Reflectance spectra for Figure 3 are available on Github (https://github.com/nelsopet/lecospec) and are archived at the ORNL DAAC (https://doi.org/10.3334/ORNLDAAC/1980). These data will also be made available on EcoSIS (https://ecosis.org/).

Reflectance spectra and hydration data for bryophytes in Figure 4 will be archived at the Arctic Data Center by NCEAS repository (https://www.nceas.ucsb.edu/arctic-data-center)

Data for Figure 5 came from Arctic Vegetation Plots in Flux Tower Footprints, North Slope, Alaska, 2014. This dataset provides spectral, carbon flux, vegetation, environmental, and soil data collected from plots located in the footprints of eddy covariance flux towers along a 300 km north-south latitudinal gradient from Barrow, to Atqasuk, and to Ivotuk across the North Slope of Alaska in 2014. Within each of the five flux tower footprints, 1x1-m quadrats were placed subjectively within widespread habitat or micro-habitat types to map the dominant vegetation communities and site environmental factors. Specific attributes included species cover data and environmental, soil and spectral data (active layer thaw depth, moss layer depth, organic horizon layer depth, standing water depth, soil moisture status, vegetation height, LAI).

Data for Figure 5 are available at NASA's Earth Observing System Data and Information System (EOSDIS) (Registration required) https://doi.org/10.3334/ORNLDAAC/1546 with additional information at https://daac.ornl.gov/ABOVE/guides/Flux_Tower_Zona_Veg_Plots.html. This dataset is openly shared, without restriction, in accordance with the EOSDIS Data Use Policy

Data for Figure 5 are cited in the text using the references below:

Davidson, S.J., and D. Zona. 2018. Arctic Vegetation Plots in Flux Tower Footprints, North Slope, Alaska, 2014. ORNL DAAC, Oak Ridge, Tennessee, USA. https://doi.org/10.3334/ORNLDAAC/1546

Davidson, S.J., Santos, M.J., Sloan, V.L., Watts, J.D., Phoenix, G.K., Oechel, W.C. and Zona, D. (2016) Mapping Arctic Tundra Vegetation Communities Using Field Spectroscopy and

Multispectral Satellite Data in North Alaska, U.S.A., Remote Sensing, 8(12), 978; https://doi.org/10.3390/rs8120978

Data presented in Figure 6 is available at the NGEE-Arctic data portal https://doi.org/10.5440/1838174

Data for Figure 6 are cited in the text using the references below:

Serbin, S. and Yang, D. 2022. Maps of Arctic vegetation leaf nitrogen concentration, albedo and plant functional type (PFT) derived from imaging spectroscopy data, Council watershed, Seward Peninsula, Alaska, 2019. Next Generation Ecosystem Experiments Arctic Data Collection, Oak Ridge National Laboratory, U.S. Department of Energy, Oak Ridge, Tennessee, USA. Dataset accessed on 6 January, 2022 at https://doi.org/10.5440/1838174.

Data archiving is underway for data presented in Figures 7 and 8 and will be made available at https://zenodo.org/. Data were collected and retrieved using PhotoSpec (Grossmann et al., 2018) installed at Delta Junction Alaska as part of NASA ABoVE project 80NSSC19M0129.

References

Aalto, J., Scherrer, D., Lenoir, J., Guisan, A., & Luoto, M. (2018). Biogeophysical controls on soil-atmosphere thermal differences: implications on warming Arctic ecosystems. *Environmental Research Letters*, *13*(7), 074003. https://doi.org/10.1088/1748-9326/aac83e

Aartsma, P., Asplund, J., Odland, A., Reinhardt, S., & Renssen, H. (2021). Microclimatic

comparison of lichen heaths and shrubs: shrubification generates atmospheric heating but subsurface cooling during the growing season. *Biogeosciences*, *18*(5), 1577–1599. https://doi.org/10.5194/bg-18-1577-2021

Adams, W. W., Zarter, C. R., Ebbert, V., & Demmig-Adams, B. (2004). Photoprotective Strategies of Overwintering Evergreens. *BioScience*, *54*(1), 41. https://doi.org/10.1641/0006-3568(2004)054[0041:PSOOE]2.0.CO;2

Anderson, J. E., Douglas, T. A., Barbato, R. A., Saari, S., Edwards, J. D., & Jones, R. M. (2019). Linking vegetation cover and seasonal thaw depths in interior Alaska permafrost terrains using remote sensing. *Remote Sensing of Environment*, *233*, 111363. https://doi.org/10.1016/j.rse.2019.111363

Andresen, C. G., & Lougheed, V. L. (2021). Arctic aquatic graminoid tundra responses to nutrient availability. *Biogeosciences*, *18*(8), 2649–2662. https://doi.org/10.5194/bg-18-2649-2021

Asner, G. P., & Martin, R. E. (2008). Spectral and chemical analysis of tropical forests: Scaling from leaf to canopy levels. *Remote Sensing of Environment*, *112*(10), 3958–3970. https://doi.org/10.1016/j.rse.2008.07.003

Asner, G. P., Martin, R. E., Anderson, C. B., & Knapp, D. E. (2015). Quantifying forest canopy traits: Imaging spectroscopy versus field survey. *Remote Sensing of Environment*, *158*, 15–27. https://doi.org/10.1016/j.rse.2014.11.011

Assmann, J. J., Myers-Smith, I. H., Kerby, J. T., Cunliffe, A. M., & Daskalova, G. N. (2020). Drone data reveal heterogeneity in tundra greenness and phenology not captured by satellites. *Environmental Research Letters*, *15*(12), 125002. https://doi.org/10.1088/1748-9326/abbf7d

Bartsch, A., Höfler, A., Kroisleitner, C., & Trofaier, A. (2016). Land cover mapping in northern high latitude permafrost regions with satellite data: Achievements and remaining challenges. *Remote Sensing*, *8*(12), 979. https://doi.org/10.3390/rs8120979

Beamish, A., Raynolds, M. K., Epstein, H., Frost, G. V., Macander, M. J., Bergstedt, H., et al. (2020). Recent trends and remaining challenges for optical remote sensing of Arctic tundra vegetation: A review and outlook. *Remote Sensing of Environment*, *246*, 111872. https://doi.org/10.1016/j.rse.2020.111872

Beamish, A. L., Coops, N., Chabrillat, S., & Heim, B. (2017). A Phenological Approach to Spectral Differentiation of Low-Arctic Tundra Vegetation Communities, North Slope, Alaska. *Remote Sensing*, *9*(11), 1200. https://doi.org/10.3390/rs9111200

Beckett, R. P., Minibayeva, F., Solhaug, K. A., & Roach, T. (2021). Photoprotection in lichens: adaptations of photobionts to high light. *The Lichenologist*, *53*(1), 21–33. https://doi.org/10.1017/S0024282920000535

Berner, L. T., Massey, R., Jantz, P., Forbes, B. C., Macias-Fauria, M., Myers-Smith, I., et al. (2020). Summer warming explains widespread but not uniform greening in the Arctic tundra biome. *Nature Communications*, *11*(1), 4621. https://doi.org/10.1038/s41467-020-18479-5

Bhatt, U. S., Walker, D. A., Raynolds, M. K., Walsh, J. E., Bieniek, P. A., Cai, L., et al. (2021). Climate drivers of Arctic tundra variability and change using an indicators framework, *16*(5), 055019. https://doi.org/10.1088/1748-9326/abe676

Bjorkman, A. D., Myers-Smith, I. H., Elmendorf, S. C., Normand, S., Rüger, N., Beck, P. S. A., et al. (2018). Plant functional trait change across a warming tundra biome. *Nature*, *562*(7725), 57–62. https://doi.org/10.1038/s41586-018-0563-7

Black, K. L., Wallace, C. A., & Baltzer, J. L. (2021). Seasonal thaw and landscape position determine foliar functional traits and whole-plant water use in tall shrubs on the low arctic tundra. *New Phytologist*, *231*(1), 94–107. https://doi.org/10.1111/nph.17375

Blok, D., Heijmans, M. M. P. D., Schaepman-Strub, G., van Ruijven, J., Parmentier, F. J. W., Maximov, T. C., & Berendse, F. (2011). The Cooling Capacity of Mosses: Controls on Water and Energy Fluxes in a Siberian Tundra Site. *Ecosystems*, *14*(7), 1055–1065. https://doi.org/10.1007/s10021-011-9463-5

Boelman, N. T., Rocha, A. V., & Shaver, G. R. (2011). Understanding burn severity sensing in Arctic tundra: exploring vegetation indices, suboptimal assessment timing and the impact of increasing pixel size. *International Journal of Remote Sensing*, *32*(22), 7033–7056. https://doi.org/10.1080/01431161.2011.611187

Bokhorst, S., Tømmervik, H., Callaghan, T. V., Phoenix, G. K., & Bjerke, J. W. (2012). Vegetation recovery following extreme winter warming events in the sub-Arctic estimated using NDVI from remote sensing and handheld passive proximal sensors. *Environmental and Experimental Botany*, *81*, 18–25. https://doi.org/10.1016/j.envexpbot.2012.02.011

Bratsch, S. N., Epstein, H. E., Buchhorn, M., & Walker, D. A. (2016). Differentiating among Four Arctic Tundra Plant Communities at Ivotuk, Alaska Using Field Spectroscopy. *Remote Sensing*, *8*(1), 51. https://doi.org/10.3390/rs8010051

Brodrick, P.G., Thompson D. R., Garay M. J., Giles, D. M., Holben, B. N., and Kalashnikova, O. V. (2021). Simultaneous characterization of wildfire smoke and surface properties with imaging spectroscopy during the FIREX-AQ field campaign. Journal of Geophysical Research - Atmospheres. In press, available at the Earth and Space Science Open Archive. https://doi.org/10.1002/essoar.10506794.1

Bubier, J. L., Rock, B. N., & Crill, P. M. (1997). Spectral reflectance measurements of boreal wetland and forest mosses. *Journal of Geophysical Research: Atmospheres*, *102*(D24), 29483–29494. https://doi.org/10.1029/97JD02316

Buchhorn, M., Raynolds, M. K., & Walker, D. A. (2016). Influence of BRDF on NDVI and biomass estimations of Alaska Arctic tundra, *11*(12), 125002. https://doi.org/10.1088/1748-9326/11/12/125002

CAVM Team. (2003). Circumpolar Arctic Vegetation Map. Anchorage, Alaska: U.S. Fish and Wildlife Service. Retrieved from http://www.arcticatlas.org/maps/themes/cp/

Cawse-Nicholson, K., Townsend, P. A., Schimel, D., Assiri, A. M., Blake, P. L., Buongiorno, M.

F., et al. (2021). NASA's surface biology and geology designated observable: A perspective on surface imaging algorithms. *Remote Sensing of Environment*, *257*, 112349. https://doi.org/10.1016/j.rse.2021.112349

Chapin, F. S. (2003). Effects of Plant Traits on Ecosystem and Regional Processes: a Conceptual Framework for Predicting the Consequences of Global Change. *Annals of Botany*, *91*(4), 455–463. https://doi.org/10.1093/aob/mcg041

Chapman, J. W., Thompson, D. R., Helmlinger, M. C., Bue, B. D., Green, R. O., Eastwood, M. L., et al. (2019). Spectral and Radiometric Calibration of the Next Generation Airborne Visible Infrared Spectrometer (AVIRIS-NG). *Remote Sensing*, *11*(18), 2129. https://doi.org/10.3390/rs11182129

Chasmer, L., Hopkinson, C., Veness, T., Quinton, W., & Baltzer, J. (2014). A decision-tree classification for low-lying complex land cover types within the zone of discontinuous permafrost. *Remote Sensing of Environment*, *143*, 73–84.

Chen, W., Tape, K. D., Euskirchen, E. S., Liang, S., Matos, A., Greenberg, J., & Fraterrigo, J. M. (2020). Impacts of Arctic Shrubs on Root Traits and Belowground Nutrient Cycles Across a Northern Alaskan Climate Gradient. *Frontiers in Plant Science*, *11*, 1943. https://doi.org/10.3389/fpls.2020.588098

Cooper, E. J. (2014). Warmer Shorter Winters Disrupt Arctic Terrestrial Ecosystems. *Annual Review of Ecology, Evolution, and Systematics*, *45*(1), 271–295. https://doi.org/10.1146/annurev-ecolsys-120213-091620

Cornelissen, J. H. C., Lang, S. I., Soudzilovskaia, N. A., & During, H. J. (2007). Comparative Cryptogam Ecology: A Review of Bryophyte and Lichen Traits that Drive Biogeochemistry. *Annals of Botany*, *99*(5), 987–1001. https://doi.org/10.1093/aob/mcm030

Cunliffe, A. M., Anderson, K., Boschetti, F., Brazier, R. E., Graham, H. A., Myers-Smith, I. H., et al. (2021). Global application of an unoccupied aerial vehicle photogrammetry protocol for predicting aboveground biomass in non-forest ecosystems. *Remote Sensing in Ecology and Conservation*, rse2.228. https://doi.org/10.1002/rse2.228

Curran, P. J., Kupiec, J. A., & Smith, G. M. (1997). Remote sensing the biochemical composition of a slash pine canopy. *IEEE Transactions on Geoscience and Remote Sensing*, *35*(2), 415–420. https://doi.org/10.1109/36.563280

Davidson, S., Santos, M., Sloan, V., Watts, J., Phoenix, G., Oechel, W., & Zona, D. (2016). Mapping Arctic Tundra Vegetation Communities Using Field Spectroscopy and Multispectral Satellite Data in North Alaska, USA. *Remote Sensing*, *8*(12), 978. https://doi.org/10.3390/rs8120978

Demmig-Adams, B., Adams III, W. W., Barker, D. H., Logan, B. A., Bowling, D. R., & Verhoeven, A. S. (1996). Using chlorophyll fluorescence to assess the fraction of absorbed light allocated to thermal dissipation of excess excitation. *Physiologia Plantarum*, *98*(2), 253–264. https://doi.org/10.1034/j.1399-3054.1996.980206.x

Dietze, M. C., Serbin, S. P., Davidson, C., Desai, A. R., Feng, X., Kelly, R., et al. (2014). A

quantitative assessment of a terrestrial biosphere model's data needs across North American biomes. *Journal of Geophysical Research: Biogeosciences*, *119*(3), 286–300. https://doi.org/10.1002/2013JG002392

Drolet, G., Wade, T., Nichol, C. J., MacLellan, C., Levula, J., Porcar-Castell, A., et al. (2014). A temperature-controlled spectrometer system for continuous and unattended measurements of canopy spectral radiance and reflectance. *International Journal of Remote Sensing*, *35*(5), 1769–1785. https://doi.org/10.1080/01431161.2014.882035

Durán, S. M., Martin, R. E., Díaz, S., Maitner, B. S., Malhi, Y., Salinas, N., et al. (2019). Informing trait-based ecology by assessing remotely sensed functional diversity across a broad tropical temperature gradient. *Science Advances*, *5*(12), eaaw8114. https://doi.org/10.1126/sciadv.aaw8114

Eitel, J. U. H., Maguire, A. J., Boelman, N., Vierling, L. A., Griffin, K. L., Jensen, J., et al. (2019). Proximal remote sensing of tree physiology at northern treeline: Do late-season changes in the photochemical reflectance index (PRI) respond to climate or photoperiod? *Remote Sensing of Environment*, *221*, 340–350. https://doi.org/10.1016/j.rse.2018.11.022

Eitel, J. U. H., Griffin, K. L., Boelman, N. T., Maguire, A. J., Meddens, A. J. H., Jensen, J., et al. (2020). Remote sensing tracks daily radial wood growth of evergreen needleleaf trees. *Global Change Biology*, *26*(7), 4068–4078. https://doi.org/10.1111/gcb.15112

Epstein, H. E., Walker, D. A., Raynolds, M. K., Jia, G. J., & Kelley, A. M. (2008). Phytomass patterns across a temperature gradient of the North American arctic tundra. *Journal of Geophysical Research: Biogeosciences*, *113*(G3). https://doi.org/10.1029/2007JG000555

Epstein, H. E., Walker, D. A., Frost, G. V., Raynolds, M. K., Bhatt, U., Daanen, R., et al. (2020). Spatial patterns of arctic tundra vegetation properties on different soils along the Eurasia Arctic Transect, and insights for a changing Arctic, *16*(1), 014008. https://doi.org/10.1088/1748-9326/abc9e3

Fer, I., Kelly, R., Moorcroft, P. R., Richardson, A. D., Cowdery, E. M., & Dietze, M. C. (2018). Linking big models to big data: efficient ecosystem model calibration through Bayesian model emulation. *Biogeosciences*, *15*(19), 5801–5830. https://doi.org/10.5194/bg-15-5801-2018

Féret, J.-B., François, C., Gitelson, A., Asner, G. P., Barry, K. M., Panigada, C., et al. (2011). Optimizing spectral indices and chemometric analysis of leaf chemical properties using radiative transfer modeling. *Remote Sensing of Environment*, *115*(10), 2742–2750. https://doi.org/10.1016/j.rse.2011.06.016

Fisher, J. B., Hayes, D. J., Schwalm, C. R., Huntzinger, D. N., Stofferahn, E., Schaefer, K., et al. (2018). Missing pieces to modeling the Arctic-Boreal puzzle. *Environmental Research Letters*, *13*(2), 020202. https://doi.org/10.1088/1748-9326/aa9d9a

French, N. H. F., Jenkins, L. K., Loboda, T. V., Flannigan, M., Jandt, R., Bourgeau-Chavez, L. L., & Whitley, M. (2015). Fire in arctic tundra of Alaska: past fire activity, future fire potential, and significance for land management and ecology. *International Journal of Wildland Fire*, *24*(8), 1045–1061. https://doi.org/10.1071/WF14167

Gamon, J. A., Peñuelas, J., & Field, C. B. (1992). A narrow-waveband spectral index that tracks diurnal changes in photosynthetic efficiency. *Remote Sensing of Environment*, *41*(1), 35–44. https://doi.org/10.1016/0034-4257(92)90059-S

Gamon, J. A., Serrano, L., & Surfus, J. S. (1997). The photochemical reflectance index: an optical indicator of photosynthetic radiation use efficiency across species, functional types, and nutrient levels. *Oecologia*, *112*(4), 492–501. https://doi.org/10.1007/s004420050337

Gamon, J. A., Somers, B., Malenovský, Z., Middleton, E. M., Rascher, U., & Schaepman, M. E. (2019). Assessing Vegetation Function with Imaging Spectroscopy. *Surveys in Geophysics*, *40*(3), 489–513. https://doi.org/10.1007/s10712-019-09511-5

Gamon, John A., Cheng, Y., Claudio, H., MacKinney, L., & Sims, D. A. (2006). A mobile tram system for systematic sampling of ecosystem optical properties. *Remote Sensing of Environment*, *103*(3), 246–254. https://doi.org/10.1016/j.rse.2006.04.006

Gamon, John A., Huemmrich, K. F., Stone, R. S., & Tweedie, C. E. (2013). Spatial and temporal variation in primary productivity (NDVI) of coastal Alaskan tundra: Decreased vegetation growth following earlier snowmelt. *Remote Sensing of Environment*, *129*, 144–153. https://doi.org/10.1016/j.rse.2012.10.030

Gamon, John A., Huemmrich, K. F., Wong, C. Y. S., Ensminger, I., Garrity, S., Hollinger, D. Y., et al. (2016). A remotely sensed pigment index reveals photosynthetic phenology in evergreen conifers. *Proceedings of the National Academy of Sciences*, *113*(46), 13087–13092. https://doi.org/10.1073/pnas.1606162113

Goswami, S., Gamon, J. A., & Tweedie, C. E. (2011). Surface hydrology of an arctic ecosystem: Multiscale analysis of a flooding and draining experiment using spectral reflectance. *Journal of Geophysical Research: Biogeosciences*, *116*(G4). https://doi.org/10.1029/2010JG001346

Granlund, L., Keski-Saari, S., Kumpula, T., Oksanen, E., & Keinänen, M. (2018). Imaging lichen water content with visible to mid-wave infrared (400–5500 nm) spectroscopy. *Remote Sensing of Environment*, *216*, 301–310. https://doi.org/10.1016/j.rse.2018.06.041

Greaves, H. E., Eitel, J. U., Vierling, L. A., Boelman, N. T., Griffin, K. L., Magney, T. S., & Prager, C. M. (2019). 20 cm resolution mapping of tundra vegetation communities provides an ecological baseline for important research areas in a changing Arctic environment. *Environmental Research Communications*, *1*(10), 105004.

Green, T. G. A., & Lange, O. L. (1995). Photosynthesis in poikilohydric plants: A comparison of lichens and bryophytes. In *Ecophysiology of Photosynthesis* (Vol. 100, pp. 319–341). Berlin, Hedelberg: Springer.

Grosse, G., Jones, B., & Arp, C. (2013). 8.21 Thermokarst Lakes, Drainage, and Drained Basins. In *Treatise on Geomorphology* (pp. 325–353). Elsevier. https://doi.org/10.1016/B978-0-12-374739-6.00216-5

Grossmann, K., Frankenberg, C., Magney, T. S., Hurlock, S. C., Seibt, U., & Stutz, J. (2018).

PhotoSpec: A new instrument to measure spatially distributed red and far-red Solar-Induced Chlorophyll Fluorescence. *Remote Sensing of Environment*, *216*, 311–327. https://doi.org/10.1016/j.rse.2018.07.002

Harley, P. C., Tenhunen, J. D., Murray, K. J., & Beyers, J. (1989). Irradiance and temperature effects on photosynthesis of tussock tundra Sphagnum mosses from the foothills of the Philip Smith Mountains, Alaska. *Oecologia*, *79*(2), 251–259. https://doi.org/10.1007/BF00388485

Harris, A., Bryant, R. G., & Baird, A. J. (2005). Detecting near-surface moisture stress in Sphagnum spp. *Remote Sensing of Environment*, *97*(3), 371–381. https://doi.org/10.1016/j.rse.2005.05.001

Harris, Angela, & Bryant, R. G. (2009). A multi-scale remote sensing approach for monitoring northern peatland hydrology: Present possibilities and future challenges. *Journal of Environmental Management*, *90*(7), 2178–2188. https://doi.org/10.1016/j.jenvman.2007.06.025

Healey, N. C., Oberbauer, S. F., Ahrends, H. E., Dierick, D., Welker, J. M., Leffler, A. J., et al. (2014). A Mobile Instrumented Sensor Platform for Long-Term Terrestrial Ecosystem Analysis: An Example Application in an Arctic Tundra Ecosystem. *Journal Of Environmental Informatics*, *24*(1), 1–10.

Heggberget, T. M., Gaare, E., & Ball, J. P. (2002). Reindeer (Rangifer tarandus) and climate change: Importance of winter forage. *Rangifer*, *22*(1), 13. https://doi.org/10.7557/2.22.1.388

Hilker, T., Gitelson, A., Coops, N. C., Hall, F. G., & Black, T. A. (2011). Tracking plant physiological properties from multi-angular tower-based remote sensing. *Oecologia*, *165*(4), 865–876. https://doi.org/10.1007/s00442-010-1901-0

Holt, E. A., & Nelson, P. R. (2021). Climatic, vegetative, and disturbance predictors of lichen species' height in Arctic Alaska, USA. *Polar Biology*, *44*(1), 133–145. https://doi.org/10.1007/s00300-020-02784-2

Holtmeier, F. K., & Broll, G. E. (2007). Treeline advance - driving processes and adverse factors. *Landscape Online*, *1*, 1–33. https://doi.org/10.3097/LO.200701

Holtmeier, F.-K., & Broll, G. (2019). Treeline Research—From the Roots of the Past to Present Time. A Review. *Forests*, *11*(1), 38. https://doi.org/10.3390/f11010038

Hope, A. S., & Stow, D. A. (1996). Shortwave Reflectance Properties of Arctic Tundra Landscapes. In *Landscape Function and Disturbance in Arctic Tundra* (Vol. 120, pp. 155–164). Berlin, Hedelberg: Springer.

Hovi, A., Raitio, P., & Rautiainen, M. (2017). A spectral analysis of 25 boreal tree species. *Silva Fennica*, *51*(4). https://doi.org/10.14214/sf.7753

Huemmrich, K. F, Gamon, J. A., Tweedie, C. E., Oberbauer, S. F., Kinoshita, G., Houston, S., et al. (2010). Remote sensing of tundra gross ecosystem productivity and light use efficiency under varying temperature and moisture conditions. *Remote Sensing of Environment*, *114*(3), 481–489. https://doi.org/10.1016/j.rse.2009.10.003

Huemmrich, Karl Fred, Gamon, J. A., Tweedie, C. E., Campbell, P. K. E., Landis, D. R., & Middleton, E. M. (2013). Arctic Tundra Vegetation Functional Types Based on Photosynthetic Physiology and Optical Properties. *IEEE Journal of Selected Topics in Applied Earth Observations and Remote Sensing*, *6*(2), 265–275. https://doi.org/10.1109/JSTARS.2013.2253446

Huemmrich, Karl Fred, Vargas Zesati, S., Campbell, P., & Tweedie, C. (n.d.). Canopy reflectance models illustrate varying NDVI responses to change in high latitude ecosystems. *Ecological Applications*, *n/a*(n/a), e02435. https://doi.org/10.1002/eap.2435

Hunt, E. R., & Rock, B. N. (1989). Detection of changes in leaf water content using Near- and Middle-Infrared reflectances. *Remote Sensing of Environment*, *30*(1), 43–54. https://doi.org/10.1016/0034-4257(89)90046-1

Jacquemoud, S., Verhoef, W., Baret, F., Bacour, C., Zarco-Tejada, P. J., Asner, G. P., et al. (2009). PROSPECT+SAIL models: A review of use for vegetation characterization. *Remote Sensing of Environment*, *113*, S56–S66. https://doi.org/10.1016/j.rse.2008.01.026

Joly, K., Jandt, R. R., Meyers, C. R., & Cole, M. J. (2007). Changes in vegetative cover on Western Arctic Herd winter range from 1981 to 2005: potential effects of grazing and climate change. *Rangifer*, 199–207. https://doi.org/10.7557/2.27.4.345

Kade, A., Walker, D. A., & Raynolds, M. K. (2005). Plant communities and soils in cryoturbated tundra along a bioclimate gradient in the Low Arctic, Alaska. *Phytocoenologia*, 761–820. https://doi.org/10.1127/0340-269X/2005/0035-0761

Karlsen, S. R., Stendardi, L., Tømmervik, H., Nilsen, L., Arntzen, I., & Cooper, E. J. (2021). Time-series of cloud-free Sentinel-2 NDVI data used in mapping the onset of growth of central Spitsbergen, Svalbard. *Remote Sensing*, *13*(15), 3031. https://doi.org/10.3390/rs13153031

Kelsey, K., C., Pedersen, S., Hojlund, Leffler, A. J., Sexton, J., O., Feng, M., & Welker, J., M. (2021). Winter snow and spring temperature have differential effects on vegetation phenology and productivity across Arctic plant communities. *Global Change Biology*, *27*, 1572–1586. https://doi.org/10.1111/gcb.15505

Kuusinen, N., Juola, J., Karki, B., Stenroos, S., & Rautiainen, M. (2020). A spectral analysis of common boreal ground lichen species. *Remote Sensing of Environment*, *247*, 111955. https://doi.org/10.1016/j.rse.2020.111955

Lang, M. W., Bourgeau-Chavez, L. L., Tiner, R. W., & Klemas, V. V. (2015). Chapter 5: Advances in Remotely Sensed Data and Techniques for Wetland Mapping and Monitoring. In *Remote Sensing of Wetlands: Applications and Advances* (pp. 79–116). Boca Raton, Florida, USA: CRC Press Taylor & Francis Group.

Lange, O. L., Hahn, S. C., Müller, G., Meyer, A., & Tenhunen, J. D. (1996). Upland tundra in the foothills of the Brooks Range, Alaska: Influence of light, water content and temperature on CO2 exchange of characteristic lichen species. *Flora*, *191*(1), 67–83. https://doi.org/10.1016/S0367-2530(17)30691-6

Langford, Z. L., Kumar, J., Hoffman, F. M., Breen, A. L., & Iversen, C. M. (2019). Arctic

Vegetation Mapping Using Unsupervised Training Datasets and Convolutional Neural Networks. *Remote Sensing*, *11*(1), 69. https://doi.org/10.3390/rs11010069

Lantz, T. C., Gergel, S. E., & Kokelj, S. V. (2010). Spatial Heterogeneity in the Shrub Tundra Ecotone in the Mackenzie Delta Region, Northwest Territories: Implications for Arctic Environmental Change. *Ecosystems*, *13*(2), 194–204. https://doi.org/10.1007/s10021-009-9310-0

Li, A., Matsuoka, N., Niu, F., Chen, J., Ge, Z., Hu, W., et al. (2021). Ice needles weave patterns of stones in freezing landscapes. *Proceedings of the National Academy of Sciences*, *118*(40). https://doi.org/10.1073/pnas.2110670118

Liu, N., Budkewitsch, P., & Treitz, P. (2017). Examining spectral reflectance features related to Arctic percent vegetation cover: Implications for hyperspectral remote sensing of Arctic tundra. *Remote Sensing of Environment*, *192*, 58–72. https://doi.org/10.1016/j.rse.2017.02.002

Luus, K. A., Commane, R., Parazoo, N. C., Benmergui, J., Euskirchen, E. S., Frankenberg, C., et al. (2017). Tundra photosynthesis captured by satellite-observed solar-induced chlorophyll fluorescence. *Geophysical Research Letters*, *44*(3), 1564–1573. https://doi.org/10.1002/2016GL070842

Macander, M. J., Frost, G. V., Nelson, P. R., & Swingley, C. S. (2017). Regional Quantitative Cover Mapping of Tundra Plant Functional Types in Arctic Alaska. *Remote Sensing*, *9*(10), 1024. https://doi.org/10.3390/rs9101024

Macander, M. J., Palm, E. C., Frost, G. V., Herriges, J. D., Nelson, P. R., Roland, C., et al. (2020). Lichen cover mapping for caribou ranges in interior Alaska and Yukon, *15*(5), 055001. https://doi.org/10.1088/1748-9326/ab6d38

Maguire, A. J., Eitel, J. U. H., Magney, T. S., Frankenberg, C., Köhler, P., Orcutt, E. L., et al. (2021). Spatial covariation between solar-induced fluorescence and vegetation indices from Arctic-Boreal landscapes. *Environmental Research Letters*, *16*(9), 095002. https://doi.org/10.1088/1748-9326/ac188a

Makoto, K., & Klaminder, J. (2012). The influence of non-sorted circles on species diversity of vascular plants, bryophytes and lichens in Sub-Arctic Tundra. *Polar Biology*, *35*(11), 1659–1667. https://doi.org/10.1007/s00300-012-1206-3

Martin, M. E., Plourde, L. C., Ollinger, S. V., Smith, M.-L., & McNeil, B. E. (2008). A generalizable method for remote sensing of canopy nitrogen across a wide range of forest ecosystems. *Remote Sensing of Environment*, *112*(9), 3511–3519. https://doi.org/10.1016/j.rse.2008.04.008

Matveyeva, N. V. (1998). Zonation in plant cover of the Arctic. *Russian Academy of Sciences, Proceedings of the Komarov Botanical Institute*, *21*, 220pp.

May, J. L., Parker, T., Unger, S., & Oberbauer, S. F. (2018). Short term changes in moisture content drive strong changes in Normalized Difference Vegetation Index and gross primary productivity in four Arctic moss communities. *Remote Sensing of Environment*, *212*, 114–120. https://doi.org/10.1016/j.rse.2018.04.041

Meireles, J. E., Cavender-Bares, J., Townsend, P. A., Ustin, S., Gamon, J. A., Schweiger, A. K., et al. (2020). Leaf reflectance spectra capture the evolutionary history of seed plants. *New Phytologist*, *228*(2), 485–493. https://doi.org/10.1111/nph.16771

Metcalfe, D. B., Hermans, T. D. G., Ahlstrand, J., Becker, M., Berggren, M., Björk, R. G., et al. (2018). Patchy field sampling biases understanding of climate change impacts across the Arctic. *Nature Ecology & Evolution*, *2*(9), 1443–1448. https://doi.org/10.1038/s41559-018-0612-5

Miller, C., Griffith, P., Goetz, S., Hoy, E., Pinto, N., McCubbin, I., et al. (2019). An overview of ABoVE airborne campaign data acquisitions and science opportunities. *Environmental Research Letters*, *14*(8), 080201.

Montesano, Paul M., Sun, G., Dubayah, R. O., & Ranson, K. J. (2016). Spaceborne potential for examining taiga–tundra ecotone form andvulnerability. *Biogeosciences*, *13*(13), 3847–3861. https://doi.org/10.5194/bg-13-3847-2016

Montesano, Paul M, Neigh, C. S. R., Macander, M., Feng, M., & Noojipady, P. (2020). The bioclimatic extent and pattern of the cold edge of the boreal forest: the circumpolar taiga-tundra ecotone. *Environmental Research Letters*, *15*(10), 105019. https://doi.org/10.1088/1748-9326/abb2c7

Montesano, Paul Mannix, Neigh, C. S. R., Sexton, J., Feng, M., Channan, S., Ranson, K. J., & Townshend, J. R. (2016). Calibration and Validation of Landsat Tree Cover in the Taiga−Tundra Ecotone. *Remote Sensing*, *8*(7), 551. https://doi.org/10.3390/rs8070551

Moorthy, I., Miller, J. R., & Noland, T. L. (2008). Estimating chlorophyll concentration in conifer needles with hyperspectral data: An assessment at the needle and canopy level. *Remote Sensing of Environment*, *112*(6), 2824–2838. https://doi.org/10.1016/j.rse.2008.01.013

Murray, K. J., Tenhunen, J. D., & Nowak, R. S. (1993). Photoinhibition as a control on photosynthesis and production of Sphagnum mosses. *Oecologia*, *96*(2), 200–207. https://doi.org/10.1007/BF00317733

Myers-Smith, I. H., Thomas, H. J. D., & Bjorkman, A. D. (2019). Plant traits inform predictions of tundra responses to global change. *New Phytologist*, *221*(4), 1742–1748. https://doi.org/10.1111/nph.15592

Myers-Smith, I. H., Kerby, J. T., Phoenix, G. K., Bjerke, J. W., Epstein, H. E., Assmann, J. J., et al. (2020). Complexity revealed in the greening of the Arctic. *Nature Climate Change*, *10*(2), 106–117.

Nelson, P. R., Roland, C., Macander, M. J., & McCune, B. (2013). Detecting continuous lichen abundance for mapping winter caribou forage at landscape spatial scales. *Remote Sensing of Environment*, *137*, 43–54. https://doi.org/10.1016/j.rse.2013.05.026

Neta, T., Cheng, Q., Bello, R. L., & Hu, B. (2010). Lichens and mosses moisture content assessment through high-spectral resolution remote sensing technology: a case study of the Hudson Bay Lowlands, Canada. *Hydrological Processes*, *24*(18), 2617–2628. https://doi.org/10.1002/hyp.7669

Nieke, J., & Rast, M. (2018). Towards the Copernicus Hyperspectral Imaging Mission For The Environment (CHIME). In *IGARSS 2018 - 2018 IEEE International Geoscience and Remote Sensing Symposium* (pp. 157–159). https://doi.org/10.1109/IGARSS.2018.8518384

Niinemets, Ü., & Tobias, M. (2014). Scaling Light Harvesting from Moss "Leaves" to Canopies. In D. T. Hanson & S. K. Rice (Eds.), *Photosynthesis in Bryophytes and Early Land Plants* (pp. 151–171). Dordrecht: Springer Netherlands. https://doi.org/10.1007/978-94-007-6988-5_9

Niittynen, P., Heikkinen, R. K., Aalto, J., Guisan, A., Kemppinen, J., & Luoto, M. (2020). Fine-scale tundra vegetation patterns are strongly related to winter thermal conditions. *Nature Climate Change*, *10*(12), 1143–1148. https://doi.org/10.1038/s41558-020-00916-4

Oechel, W. C., Hastings, S. J., Vourlrtis, G., Jenkins, M., Riechers, G., & Grulke, N. (1993). Recent change of Arctic tundra ecosystems from a net carbon dioxide sink to a source. *Nature*, *361*(6412), 520–523. https://doi.org/10.1038/361520a0

Ollinger, S. V., & Smith, M.-L. (2005). Net Primary Production and Canopy Nitrogen in a Temperate Forest Landscape: An Analysis Using Imaging Spectroscopy, Modeling and Field Data. *Ecosystems*, *8*(7), 760–778. https://doi.org/10.1007/s10021-005-0079-5

Olofsson, J., Tømmervik, H., & Callaghan, T. V. (2012). Vole and lemming activity observed from space. *Nature Climate Change*, *2*(12), 880–883. https://doi.org/10.1038/nclimate1537

Parazoo, N. C., Arneth, A., Pugh, T. A. M., Smith, B., Steiner, N., Luus, K., et al. (2018). Spring photosynthetic onset and net CO2 uptake in Alaska triggered by landscape thawing. *Global Change Biology*, *24*(8), 3416–3435. https://doi.org/10.1111/gcb.14283

Patankar, R., Mortazavi, B., Oberbauer, S. F., & Starr, G. (2013). Diurnal patterns of gas-exchange and metabolic pools in tundra plants during three phases of the arctic growing season. *Ecology and Evolution*, *3*(2), 375–388. https://doi.org/10.1002/ece3.467

Petzold, D. E., & Goward, S. N. (1988). Reflectance spectra of subarctic lichens. *Remote Sensing of Environment*, *24*(3), 481–492. https://doi.org/10.1016/0034-4257(88)90020-X

Pierrat, Z., Nehemy, M. F., Roy, A., Magney, T., Parazoo, N. C., Laroque, C., et al. (2021). Tower-Based Remote Sensing Reveals Mechanisms Behind a Two-phased Spring Transition in a Mixed-Species Boreal Forest. *Journal of Geophysical Research: Biogeosciences*, *126*(5), e2020JG006191. https://doi.org/10.1029/2020JG006191

Puletti, N., Camarretta, N., & Corona, P. (2016). Evaluating EO1-Hyperion capability for mapping conifer and broadleaved forests. *European Journal of Remote Sensing*, *49*(1), 157–169. https://doi.org/10.5721/EuJRS20164909

Räsänen, A., & Virtanen, T. (2019). Data and resolution requirements in mapping vegetation in spatially heterogeneous landscapes. *Remote Sensing of Environment*, *230*, 111207. https://doi.org/10.1016/j.rse.2019.05.026

Rautiainen, M., Mõttus, M., Heiskanen, J., Akujärvi, A., Majasalmi, T., & Stenberg, P. (2011).

Seasonal reflectance dynamics of common understory types in a northern European boreal forest. *Remote Sensing of Environment*, *115*(12), 3020–3028. https://doi.org/10.1016/j.rse.2011.06.005

Raynolds, M. K., Walker, D. A., Balser, A., Bay, C., Campbell, M., Cherosov, M. M., et al. (2019). A raster version of the Circumpolar Arctic Vegetation Map (CAVM). *Remote Sensing of Environment*, *232*, 111297.

Rees, W. G., Tutubalina, O. V., & Golubeva, E. I. (2004). Reflectance spectra of subarctic lichens between 400 and 2400 nm. *Remote Sensing of Environment*, *90*(3), 281–292. https://doi.org/10.1016/j.rse.2003.12.009

Rogers, A., Medlyn, B. E., Dukes, J. S., Bonan, G., von Caemmerer, S., Dietze, M. C., et al. (2017). A roadmap for improving the representation of photosynthesis in Earth system models. *New Phytologist*, *213*(1), 22–42. https://doi.org/10.1111/nph.14283

Schaepman, M. E., Ustin, S. L., Plaza, A. J., Painter, T. H., Verrelst, J., & Liang, S. (2009). Earth system science related imaging spectroscopy—An assessment. *Remote Sensing of Environment*, *113*, S123–S137. https://doi.org/10.1016/j.rse.2009.03.001

Schimel, D., Pavlick, R., Fisher, J. B., Asner, G. P., Saatchi, S., Townsend, P., et al. (2015). Observing terrestrial ecosystems and the carbon cycle from space. *Global Change Biology*, *21*(5), 1762–1776. https://doi.org/10.1111/gcb.12822

Serbin, S. P., & Townsend, P. A. (2020). Scaling Functional Traits from Leaves to Canopies. In J. Cavender-Bares, J. A. Gamon, & P. A. Townsend (Eds.), *Remote Sensing of Plant Biodiversity* (pp. 43–82). Cham: Springer International Publishing. https://doi.org/10.1007/978-3-030-33157-3_3

Serbin, S. P., Wu, J., Ely, K. S., Kruger, E. L., Townsend, P. A., Meng, R., et al. (2019). From the Arctic to the tropics: multibiome prediction of leaf mass per area using leaf reflectance. *New Phytologist*, *224*(4), 1557–1568. https://doi.org/10.1111/nph.16123

Shaver, G. R. (1981). Mineral nutrition and leaf longevity in an evergreen shrub, Ledum palustre ssp. decumbens. *Oecologia*, *49*(3), 362–365. https://doi.org/10.1007/BF00347599

Shiklomanov, A. N., Bradley, B. A., Dahlin, K. M., M Fox, A., Gough, C. M., Hoffman, F. M., et al. (2019). Enhancing global change experiments through integration of remote-sensing techniques. *Frontiers in Ecology and the Environment*, *17*(4), 215–224. https://doi.org/10.1002/fee.2031

Shiklomanov, A. N., Dietze, M. C., Fer, I., Viskari, T., & Serbin, S. P. (2021). Cutting out the middleman: calibrating and validating a dynamic vegetation model (ED2-PROSPECT5) using remotely sensed surface reflectance. *Geoscientific Model Development*, *14*(5), 2603–2633. https://doi.org/10.5194/gmd-14-2603-2021

Shur, Y. L., & Jorgenson, M. T. (2007). Patterns of permafrost formation and degradation in relation to climate and ecosystems. *Permafrost and Periglacial Processes*, *18*(1), 7–19. https://doi.org/10.1002/ppp.582

Singh, A., Serbin, S. P., McNeil, B. E., Kingdon, C. C., & Townsend, P. A. (2015). Imaging

spectroscopy algorithms for mapping canopy foliar chemical and morphological traits and their uncertainties. *Ecological Applications*, *25*(8), 2180–2197. https://doi.org/10.1890/14-2098.1

Smith, C. W., Panda, S. K., Bhatt, U. S., & Meyer, F. J. (2021). Improved Boreal Forest Wildfire Fuel Type Mapping in Interior Alaska Using AVIRIS-NG Hyperspectral Data. *Remote Sensing*, *13*(5), 897.

Spribille, T., Tuovinen, V., Resl, P., Vanderpool, D., Wolinski, H., Aime, M. C., et al. (2016). Basidiomycete yeasts in the cortex of ascomycete macrolichens. *Science*, *353*(6298), 488–492. https://doi.org/10.1126/science.aaf8287

Starr, G., & Oberbauer, S. F. (2003). Photosynthesis of Arctic Evergreens Under Snow: Implications for Tundra Ecosystem Carbon Balance. *Ecology*, *84*(6), 1415–1420. https://doi.org/10.1890/02-3154

Stasinski, L., White, D. M., Nelson, P. R., Ree, R. H., & Meireles, J. E. (n.d.). Reading light: leaf spectra capture fine-scale diversity of closely related, hybridizing arctic shrubs. *New Phytologist*, *n/a*(n/a). https://doi.org/10.1111/nph.17731

Stow, D. A., Burns, B. H., & Hope, A. S. (1993). Spectral, spatial and temporal characteristics of Arctic tundra reflectance. *International Journal of Remote Sensing*, *14*(13), 2445–2462. https://doi.org/10.1080/01431169308904285

Stumberg, N., Bollandsås, O., Gobakken, T., & Næsset, E. (2014). Automatic Detection of Small Single Trees in the Forest-Tundra Ecotone Using Airborne Laser Scanning. *Remote Sensing*, *6*(10), 10152–10170. https://doi.org/10.3390/rs61010152

Sturm, M., Schimel, J., Michaelson, G., Welker, J. M., Oberbauer, S. F., Liston, G. E., et al. (2005). Winter Biological Processes Could Help Convert Arctic Tundra to Shrubland. *BioScience*, *55*(1), 17–26. https://doi.org/10.1641/0006-3568(2005)055[0017:WBPCHC]2.0.CO;2

Sulla-Menashe, D., Gray, J. M., Abercrombie, S. P., & Friedl, M. A. (2019). Hierarchical mapping of annual global land cover 2001 to present: The MODIS Collection 6 Land Cover product. *Remote Sensing of Environment*, *222*, 183–194.

Tang, Z., Xu, W., Zhou, G., Bai, Y., Li, J., Tang, X., et al. (2018). Patterns of plant carbon, nitrogen, and phosphorus concentration in relation to productivity in China's terrestrial ecosystems. *Proceedings of the National Academy of Sciences*, *115*(16), 4033–4038. https://doi.org/10.1073/pnas.1700295114

Tedesco, M. (Ed.). (2015). *Remote Sensing of the Cryosphere* (1st ed.). West Sussex, United Kingdom: John Wiley & Sons Ltd.

Tenhunen, J. D., Siegwolf, R. T. W., & Oberbauer, S. F. (1995). Effects of Phenology, Physiology, and Gradients in Community Composition, Structure, and Microclimate on Tundra Ecosystem CO2 Exchange. In E.-D. Schulze & M. M. Caldwell (Eds.), *Ecophysiology of Photosynthesis* (pp. 431–460). Berlin, Heidelberg: Springer. https://doi.org/10.1007/978-3-642-79354-7_21

Thomas, H. J. D., Bjorkman, A. D., Myers-Smith, I. H., Elmendorf, S. C., Kattge, J., Diaz, S., et

al. (2020). Global plant trait relationships extend to the climatic extremes of the tundra biome. *Nature Communications*, *11*(1), 1351. https://doi.org/10.1038/s41467-020-15014-4

Thompson, D. R., Boardman, J. W., Eastwood, M. L., & Green, R. O. (2017). A large airborne survey of Earth's visible-infrared spectral dimensionality. *Optics Express*, *25*(8), 9186–9195. https://doi.org/10.1364/OE.25.009186

Thompson, D. R., Natraj, V., Green, R. O., Helmlinger, M. C., Gao, B.-C., & Eastwood, M. L. (2018). Optimal estimation for imaging spectrometer atmospheric correction. *Remote Sensing of Environment*, *216*, 355–373. https://doi.org/10.1016/j.rse.2018.07.003

Thomson, E. R., Spiegel, M. P., Althuizen, I. H., Bass, P., Chen, S., Chmurzynski, A., et al. (2021). Multiscale mapping of plant functional groups and plant traits in the High Arctic using field spectroscopy, UAV imagery and Sentinel-2A data. *Environmental Research Letters*, *16*(5), 055006.

Ustin, S. L., & Middleton, E. M. (2021). Current and near-term advances in Earth observation for ecological applications. *Ecological Processes*, *10*(1), 1. https://doi.org/10.1186/s13717-020-00255-4

Van Gaalen, K. E., Flanagan, L. B., & Peddle, D. R. (2007). Photosynthesis, chlorophyll fluorescence and spectral reflectance in Sphagnum moss at varying water contents. *Oecologia*, *153*(1), 19–28. https://doi.org/10.1007/s00442-007-0718-y

Verhoeven, A. (2014). Sustained energy dissipation in winter evergreens. *New Phytologist*, *201*(1), 57–65. https://doi.org/10.1111/nph.12466

Vickers, H., Karlsen, S. R., & Malnes, E. (2020). A 20-year MODIS-based snow cover dataset for Svalbard and its link to phenological timing and sea ice variability. *Remote Sensing*, *12*(7). https://doi.org/10.3390/rs12071123

Violle, C., Navas, M.-L., Vile, D., Kazakou, E., Fortunel, C., Hummel, I., & Garnier, E. (2007). Let the concept of trait be functional! *Oikos*, *116*(5), 882–892. https://doi.org/10.1111/j.0030-1299.2007.15559.x

Virtanen, T., & Ek, M. (2014). The fragmented nature of tundra landscape. *International Journal of Applied Earth Observation and Geoinformation*, *27*, 4–12. https://doi.org/10.1016/j.jag.2013.05.010

Vogelmann, J. E., & Moss, D. M. (1993). Spectral reflectance measurements in the genus Sphagnum. *Remote Sensing of Environment*, *45*(3), 273–279. https://doi.org/10.1016/0034-4257(93)90110-J

Walker, D. A., Jia, G. J., Epstein, H. E., Raynolds, M. K., Chapin III, F. S., Copass, C., et al. (2003). Vegetation-soil-thaw-depth relationships along a low-arctic bioclimate gradient, Alaska: synthesis of information from the ATLAS studies. *Permafrost and Periglacial Processes*, *14*(2), 103–123. https://doi.org/10.1002/ppp.452

Walker, Donald A., Raynolds, M. K., Daniëls, F. J. A., Einarsson, E., Elvebakk, A., Gould, W. A., et al. (2005). The Circumpolar Arctic vegetation map. *Journal of Vegetation Science*, *16*(3), 267–282. https://doi.org/10.1111/j.1654-1103.2005.tb02365.x

Walter, H. (1931). *Die Hydratur Der Pflanze Und Ihre Physiologisch-Okologische Bedeutung*. Jena, Germany: Fischer.

Walther, S., Voigt, M., Thum, T., Gonsamo, A., Zhang, Y., Köhler, P., et al. (2016). Satellite chlorophyll fluorescence measurements reveal large-scale decoupling of photosynthesis and greenness dynamics in boreal evergreen forests. *Global Change Biology*, *22*(9), 2979–2996. https://doi.org/10.1111/gcb.13200

Walther, S., Guanter, L., Heim, B., Jung, M., Duveiller, G., Wolanin, A., & Sachs, T. (2018). Assessing the dynamics of vegetation productivity in circumpolar regions with different satellite indicators of greenness and photosynthesis. *Biogeosciences*, *15*(20), 6221–6256. https://doi.org/10.5194/bg-15-6221-2018

Wang, J., Chen, J. M., Feng, L., Xu, J., & Zhang, F. (2020). Redefining the Directional-Hemispherical Reflectance and Transmittance of Needle-Shaped Leaves to Address Issues in Their Existing Measurement Methods. *Photogrammetric Engineering & Remote Sensing*, *86*(10), 627–641. https://doi.org/10.14358/PERS.86.10.627

Wang, J. A., & Friedl, M. A. (2019). The role of land cover change in Arctic-Boreal greening and browning trends. *Environmental Research Letters*, *14*(12), 125007. https://doi.org/10.1088/1748-9326/ab5429

Wang, J. A., Sulla-Menashe, D., Woodcock, C. E., Sonnentag, O., Keeling, R. F., & Friedl, M. A. (2020). Extensive land cover change across Arctic–Boreal Northwestern North America from disturbance and climate forcing. *Global Change Biology*, *26*(2), 807–822. https://doi.org/10.1111/gcb.14804

Wang, Z., Townsend, P. A., Schweiger, A. K., Couture, J. J., Singh, A., Hobbie, S. E., & Cavender-Bares, J. (2019). Mapping foliar functional traits and their uncertainties across three years in a grassland experiment. *Remote Sensing of Environment*, *221*, 405–416. https://doi.org/10.1016/j.rse.2018.11.016

Wang, Z., Chlus, A., Geygan, R., Ye, Z., Zheng, T., Singh, A., et al. (2020). Foliar functional traits from imaging spectroscopy across biomes in eastern North America. *New Phytologist*, *228*(2), 494–511. https://doi.org/10.1111/nph.16711

Wold, S., Sjöström, M., & Eriksson, L. (2001). PLS-regression: a basic tool of chemometrics. *Chemometrics and Intelligent Laboratory Systems*, *58*(2), 109–130. https://doi.org/10.1016/S0169-7439(01)00155-1

Wong, C. Y. S., & Gamon, J. A. (2015a). The photochemical reflectance index provides an optical indicator of spring photosynthetic activation in evergreen conifers. *New Phytologist*, *206*(1), 196–208. https://doi.org/10.1111/nph.13251

Wong, C. Y. S., & Gamon, J. A. (2015b). Three causes of variation in the photochemical reflectance index (PRI) in evergreen conifers. *New Phytologist*, *206*(1), 187–195. https://doi.org/10.1111/nph.13159

Wong, C. Y. S., D'Odorico, P., Arain, M. A., & Ensminger, I. (2020). Tracking the phenology of

photosynthesis using carotenoid-sensitive and near-infrared reflectance vegetation indices in a temperate evergreen and mixed deciduous forest. *New Phytologist*, *226*(6), 1682–1695. https://doi.org/10.1111/nph.16479

Woodward, F. I., & Diament, A. D. (1991). Functional Approaches to Predicting the Ecological Effects of Global Change. *Functional Ecology*, *5*(2), 202–212. https://doi.org/10.2307/2389258

Wullschleger, S. D., Epstein, H. E., Box, E. O., Euskirchen, E. S., Goswami, S., Iversen, C. M., et al. (2014). Plant functional types in Earth system models: past experiences and future directions for application of dynamic vegetation models in high-latitude ecosystems. *Annals of Botany*, *114*(1), 1–16. https://doi.org/10.1093/aob/mcu077

Xiao, J., Fisher, J. B., Hashimoto, H., Ichii, K., & Parazoo, N. C. (2021). Emerging satellite observations for diurnal cycling of ecosystem processes. *Nature Plants*, *7*(7), 877–887. https://doi.org/10.1038/s41477-021-00952-8

Xu, X., & Trugman, A. T. (2021). Trait-Based Modeling of Terrestrial Ecosystems: Advances and Challenges Under Global Change. *Current Climate Change Reports*, *7*(1), 1–13. https://doi.org/10.1007/s40641-020-00168-6

Yang, D., Meng, R., Morrison, B. D., McMahon, A., Hantson, W., Hayes, D. J., et al. (2020). A Multi-Sensor Unoccupied Aerial System Improves Characterization of Vegetation Composition and Canopy Properties in the Arctic Tundra. *Remote Sensing*, *12*(16), 2638. https://doi.org/10.3390/rs12162638

Yang, D., Morrison, B. D., Hantson, W., Breen, A. L., McMahon, A., Li, Q., et al. (2021). Landscape-scale characterization of Arctic tundra vegetation composition, structure, and function with a multi-sensor unoccupied aerial system, *16*(8), 085005. https://doi.org/10.1088/1748-9326/ac1291

Zakharova, L., Meyer, K. M., & Seifan, M. (2019). Trait-based modelling in ecology: A review of two decades of research. *Ecological Modelling*, *407*, 108703. https://doi.org/10.1016/j.ecolmodel.2019.05.008

Zhang, W., Miller, P. A., Jansson, C., Samuelsson, P., Mao, J., & Smith, B. (2018). Self-Amplifying Feedbacks Accelerate Greening and Warming of the Arctic. *Geophysical Research Letters*, *45*(14), 7102–7111. https://doi.org/10.1029/2018GL077830